Cellular/Molecular

Cell-Type-Specific *Shank2* Deletion in Mice Leads to Differential Synaptic and Behavioral Phenotypes

Ryunhee Kim,[1]* Jihye Kim,[2]* Changuk Chung,[2]* Seungmin Ha,[1] Seungjoon Lee,[1] Eunee Lee,[2] Ye-Eun Yoo,[1] Woohyun Kim,[1] Wangyong Shin,[1] and Eunjoon Kim[1,2]

[1]Department of Biological Sciences, Korea Advanced Institute for Science and Technology, Daejeon 305-701, Korea, and [2]Center for Synaptic Brain Dysfunctions, Institute for Basic Science, Daejeon 305-701, Korea

Shank2 is an excitatory postsynaptic scaffolding protein implicated in synaptic regulation and psychiatric disorders including autism spectrum disorders. Conventional *Shank2*-mutant (*Shank2*$^{-/-}$) mice display several autistic-like behaviors, including social deficits, repetitive behaviors, hyperactivity, and anxiety-like behaviors. However, cell-type-specific contributions to these behaviors have remained largely unclear. Here, we deleted *Shank2* in specific cell types and found that male mice lacking Shank2 in excitatory neurons (*CaMKII-Cre;Shank2*$^{fl/fl}$) show social interaction deficits and mild social communication deficits, hyperactivity, and anxiety-like behaviors. In particular, male mice lacking Shank2 in GABAergic inhibitory neurons (*Viaat-Cre;Shank2*$^{fl/fl}$) display social communication deficits, repetitive self-grooming, and mild hyperactivity. These behavioral changes were associated with distinct changes in hippocampal and striatal synaptic transmission in the two mouse lines. These results indicate that cell-type-specific deletions of *Shank2* in mice lead to differential synaptic and behavioral abnormalities.

Key words: autism; cell type; excitatory; inhibitory; Shank2; synapse

Significance Statement

Shank2 is an abundant excitatory postsynaptic scaffolding protein implicated in the regulation of excitatory synapses and diverse psychiatric disorders including autism spectrum disorders. Previous studies have reported *in vivo* functions of Shank2 mainly using global *Shank2*-null mice, but it remains largely unclear how individual cell types contribute to Shank2-dependent regulation of neuronal synapses and behaviors. Here, we have characterized conditional *Shank2*-mutant mice carrying the *Shank2* deletion in excitatory and inhibitory neurons. These mouse lines display distinct alterations of synaptic transmission in the hippocampus and striatum that are associated with differential behavioral abnormalities in social, repetitive, locomotor, and anxiety-like domains.

Introduction

Members of the Shank/ProSAP family of excitatory postsynaptic scaffolding proteins (Shank1, Shank2, and Shank3) are thought to regulate multiprotein complex assembly in the postsynaptic density of excitatory synapses and excitatory synaptic transmission, plasticity, and signaling (Sheng and Sala, 2001; Boeckers et al., 2002; Sheng and Hoogenraad, 2007; Grabrucker et al., 2011; Sheng and Kim, 2011; Jiang and Ehlers, 2013; Sala et al., 2015; Zhu et al., 2016; Monteiro and Feng, 2017).

Shank2/ProSAP1 contains multiple domains for protein–protein interactions (Du et al., 1998; Boeckers et al., 1999b; Lim et al., 1999; Naisbitt et al., 1999; Sheng and Kim, 2000), which link Shank2 to other synaptic proteins, including GKAP/SAPAP, Homer, cortactin, βPIX, IRSp53, Abp1, Abi-1, and syndapin I (Naisbitt et al., 1999; Tu et al., 1999; Boeckers et al., 1999a,b; Bockmann et al., 2002; Soltau et al., 2002; Park et al., 2003; Qualmann et al., 2004; Romorini et al., 2004; Uemura et al., 2004; Proepper et al., 2007; Hayashi et al., 2009; Schneider et al., 2014; MacGillavry et al., 2016). Shank2 is expressed in diverse rodent brain regions (Du et al., 1998; Lim et al., 1999; Boeckers et al., 1999a,b) and is mainly present at excitatory synapses (Boeckers et al., 1999b; Tao-Cheng et al., 2015; Heise et al., 2016).

More recently, *SHANK2* has been linked to several psychiatric disorders, including autism spectrum disorders (ASDs), intellectual disability, developmental delay, and schizophrenia (Pinto et

Received Sept. 18, 2017; revised Feb. 27, 2018; accepted March 10, 2018.

Author contributions: R.K., J.K., C.C., and E.K. designed research; R.K., J.K., C.C., S.H., S.L., Y.-E.Y., W.K., and W.S. performed research; S.L. and E.L. contributed unpublished reagents/analytic tools; R.K., J.K., C.C., and S.H. analyzed data; E.K. wrote the paper.

This work was supported by the National Research Foundation (NRF Global PhD Fellowship Program Grant NRF-2015H1A2A1033937 to R.K., Grant NRF-2013H1A2A1032785 to S.H., and Grant NRF-2013-Fostering Core Leaders of the Future Basic Science Program to C.C.) and the Institute for Basic Science (Grant IBS-R002-D1 to E.K.).

The authors declare no competing financial interests.

*R.K., J.K., and C.C. contributed equally to this work.

Correspondence should be addressed to Eunjoon Kim, Center for Synaptic Brain Dysfunctions, Institute for Basic Science (IBS), Daejeon 305-701, Korea. E-mail: kime@kaist.ac.kr.

DOI:10.1523/JNEUROSCI.2684-17.2018

 0270-6474/18/384076-17$15.00/0

al., 2010; Wischmeijer et al., 2011; Berkel et al., 2012; Leblond et al., 2012; Prasad et al., 2012; Rauch et al., 2012; Sanders et al., 2012; Chilian et al., 2013; Schluth-Bolard et al., 2013; Leblond et al., 2014; Costas, 2015; Peykov et al., 2015a,b; Homann et al., 2016; see also related reviews (Grabrucker et al., 2011; Jiang and Ehlers, 2013; Grabrucker, 2014; Guilmatre et al., 2014; Yoo et al., 2014; Wang et al., 2014a; Harony-Nicolas et al., 2015; Sala et al., 2015; Schmeisser, 2015; Hulbert and Jiang, 2016; Monteiro and Feng, 2017).

Mice expressing virally delivered mutant forms of Shank2 display reduced excitatory synaptic transmission and impaired cognition (Berkel et al., 2012). In addition, *Shank2*$^{-/-}$ mice with specific exon deletions (exon 7 or exons 6 and 7) display diverse autistic-like behaviors, including social deficits, repetitive behaviors, hyperactivity, and anxiety-like behaviors (Schmeisser et al., 2012; Won et al., 2012; Ey et al., 2013). Pharmacological NMDA receptor (NMDAR) activation rescues the social deficits observed in *Shank2*$^{-/-}$ (exons 6 and 7) mice (Won et al., 2012; Lee et al., 2015b), implicating NMDAR dysfunction in the phenotypes (Lee et al., 2015a). Moreover, inhibitory synaptic and Purkinje cell dysfunctions have been shown to underlie *Shank2* knock-out (KO) phenotypes (Ha et al., 2016; Peter et al., 2016; Lim et al., 2017). Most recently, mice carrying another *Shank2* deletion (exon 24) have been shown to display altered NMDA and AMPA receptor functions and mania-like behaviors that are rescued by the mood stabilizers lithium and valproic acid (Pappas et al., 2017).

Here, we attempted *Shank2* deletion restricted to CaMKIIα-positive excitatory neurons and Viaat (vesicular inhibitory amino acid transporter)-positive global GABAergic inhibitory neurons and found that these mice display distinct synaptic alterations in different brain regions and differential behavioral abnormalities in social, repetitive, locomotor, and anxiety-like domains.

Materials and Methods

Animals. To generate *Shank2*-conditional KO (cKO) mouse lines with deletion of exons 6 and 7, male homozygous *Shank2*$^{fl/fl}$ mice under the genetic background of C57BL/6J (Biocytogen) were crossed with female *Shank2*$^{fl/+}$ mice (for CaMKII and Viaat conditional) carrying the Cre transgene. Heterozygous *Shank2*$^{fl/+}$ mice were generated by crossing female cassette Shank2 (Shank2$^{cassette/+}$) mice carrying a targeted *Shank2* allele under the genetic background of C57BL/6J with male protamine-Flp mice, as described previously (Ha et al., 2016). *CaMKIIα-Cre* (#5359) and *Viaat-Cre* (#17535) mouse lines under the genetic background of C57BL × BALB/c and FVB/N, respectively, were obtained from The Jackson Laboratory. Through the cross-breeding procedures for the production of cKO mice, the Cre mouse lines used in the present study were crossed with C57BL/6J for more than five generations. To verify Cre expression patterns in the brain, *CaMKIIα-Cre* and *Viaat-Cre* mice were crossed with ROSA-tdTomato Cre reporter (JAX #7909) mice. Cre-negative *Shank2*$^{fl/fl}$ littermates were used as control groups in all experiments. *Shank2*$^{-/-}$ mice were generated as described previously (Won et al., 2012). Mice were housed and bred at the mouse facility of Korea Advanced Institute of Science and Technology (KAIST) and maintained according to the guidelines of the Animal Research Requirements of KAIST. All animals were fed *ad libitum* and housed under a 12 h light/dark cycle (light phase during 1:00 A.M. to 1:00 P.M.). Mice were weaned at the age of postnatal day 21–24. After weaning, mixed-genotype littermate mice were group housed (five to eight mice per cage) until experiments. PCR genotyping of *CaMKII/Viaat* cKO mice was performed using the following two set of oligonucleotide primers: set for floxed (367 bp) or WT allele (253 bp), forward, 5′-CGC ACT GTG GGC TCA TCA GAT G-3′, reverse, 5′-CAG ACG CAT CTT CCA GGG AAG C-3′; set for cre allele (272 bp), forward, 5′-GTG TTG CCG CGC CAT CTG C-3′, reverse, 5′-CAC CAT TGC CCC TGT TTC ACT ATC-3′. Male mice were used for all behavioral and immunoblotting experiments, whereas female mice were used for immunohistochemical staining and electrophysiological experiments (for details, see Fig. 2-1, available at https://doi.org/10.1523/JNEUROSCI.2684-17.2018.f2-1). This was partly because we attempted to best match the genders of the mice in the present study to those that we used in our previous experiments for conventional Shank2 KO mice (Won et al., 2012) for better comparisons.

Western blot analysis. Total brain lysates separated in electrophoresis and transferred to a nitrocellulose membrane were incubated with the following primary antibodies: Shank2 (1:1000, Synaptic Systems catalog #162 202, RRID:AB_2619860), α-tubulin (1:1000, Sigma-Aldrich catalog #T5168, RRID:AB_477579), Shank1 (#2100, Ha et al., 2016); and Shank3 (#2036, Lee et al., 2015c) at 4°C overnight or at room temperature for 1 h. Immunoblot images were captured using the Odyssey Fc imaging system (LI-COR Biosciences).

Immunohistochemistry. Adult mice were transcardially perfused with 0.9% saline and low pH fixative (1% paraformaldehyde in 100 mM Na-acetate buffer, pH 6.0). After overnight postfixation, brains were slowly and carefully sectioned in 60~100 μm with a vibratome and washed in phosphate buffer. After washing in TBS for 10 min, brain sections were blocked for 1 h in 10% or 2% goat serum plus 0.2% Triton X-100 in TBS. Brain sections were incubated with primary antibodies (Shank2, Synaptic Systems catalog #162 202, RRID:AB_2619860 rabbit and 162 204, RRID:AB_2619861 guinea pig), which were diluted at 1:500 to 1000 in incubation buffer (2% goat serum, 0.1% Triton X-100 in TBS) overnight at room temperature (or 48 h at 4°C) and washed 3–5 times for 10 min in TBS. After incubation with Alexa Fluor 594-conjugated secondary antibodies (Jackson ImmunoResearch Laboratories catalog #711-585-152, RRID:AB_2340621) at room temperature for 2 h (or 48 h at 4°C), sections were washed 3–5 times for 10 min in TBS. Brain sections were mounted with Vectashield using DAPI (Vector Laboratories catalog #H-1200, RRID:AB_2336790). Brain sections were imaged with a confocal microscope (10× and 63× objectives; LSM780, Carl Zeiss).

Behavioral assays. Behavioral experiments were performed in the following order: open-field test, repetitive behavioral test and/or hole-board test, three-chamber test and/or USV test, elevated plus maze and/or light–dark test, and Laboratory Animal Behavior Observation Registration and Analysis System (LABORAS) test. All behavioral assays were performed using male mice.

Three-chamber test. The three-chamber social interaction test was performed as described previously (Silverman et al., 2010; Won et al., 2012). Specifically, mice were isolated in a single cage for 4 d before the test, whereas the age-matched stranger mice (129S1/SvlmJ strain) were group housed (4–6 mice per cage). The test consisted of three phases: empty–empty (habituation), stranger 1–object (S1-O), and stranger 1 (familiar stranger)–stranger 2 (new stranger) (S1–S2) phases. The test was conducted after 30 min of habituation in an experimental booth. The white acrylic three-chambered apparatus (40 × 20 × 25 cm) included two small containers for an object or a stranger mouse in the upper or lower corner of the two side chambers. The light condition for the three-chamber test was ~70 lux. In the first habituation phase, a test mouse was placed in the center area of the three-chambered apparatus and allowed to explore the environment freely for 10 min. In the second S1-O phase that followed without an interphase interval, a stranger mouse (S1) and an inanimate blue cylindrical object (O) were placed in the two corner containers. A stranger mouse was randomly positioned in the left or right chamber. The test mouse was allowed to explore the stranger mouse or the object freely. In the third S1–S2 phase that followed without an interphase interval, the object was replaced with a new stranger mouse (S2). The test mouse was allowed to explore and interact freely with both stranger mice. For the analysis, sniffing times were measured using Ethovision XT 10 software (Noldus, RRID:SCR_000441). Sniffing was defined as the nose part of the test mouse being positioned within 2 cm from a container. The social preference index was defined as S1-O (or S2–S1)/the sum of the two parameters × 100.

Ultrasonic vocalizations (USVs). To measure USVs during courtship behavior, unfamiliar female adult mice were used as strangers/intruders. Male adult subject mice were socially isolated in their home cages for 3 d

before the test, whereas age-matched female adult stranger mice (C57BL/6J) were group housed (4–6 mice per cage). The test was conducted after 30 min of habituation in an experimental booth. A subject male mouse was placed in a testing cage under a light condition of ~60 lux for 5 min to record its basal USVs without a female stranger/intruder. Next, a randomly chosen female stranger mouse was introduced into the cage and the mice were allowed to interact with each other freely while courtship USVs of the subject mouse were recorded for 5 min. Avisoft SASLab Pro software (RRID:SCR_014438) was used to analyze USVs. Signals were filtered from 1 Hz to 100 kHz and digitized with a sampling frequency of 250 kHz, 16 bits per sample (Avisoft UltraSoundGate 116H). To generate spectrograms, the following parameters were used: FFT length: 256, frame size: 100, window: FlatTop, overlap: 75%, resulting in a frequency resolution of 977 Hz and a temporal resolution of 0.256 ms. Frequencies lower than 45 kHz were filtered out to reduce background white noises. The duration of male–female direct social interaction, defined by the total time spent sniffing, following, and mounting, was measured manually by trained experimenters in a blinded fashion. Social interactions during USV measurements were assessed exclusively in males. We did not determine whether measured USVs were from male or female mice because USVs under the context of male–female encounter, which likely represent courtship USVs, are mainly produced by males (Maggio and Whitney, 1985; Egnor and Seagraves, 2016). We did not measure female cycles, assuming that group housing may synchronize the cycles.

Repetitive behaviors. Mice were placed in a new home cage with bedding for 15–20 min. Behaviors during the time period of 5–15 min were used to measure self-grooming, digging, and jumping. A skilled experimenter scored the duration of each behavior in a blinded manner. Self-grooming was defined as stroking or scratching of the face or body or licking of body parts. Digging was defined as the behavior to dig out beddings using its head or forelimbs. Jumping was defined as the behavior of a mouse in which both of the two hind limbs simultaneously push against the ground.

Hole-board test. The hole-board apparatus (40 × 40 × 35 cm) was made of white acrylic plates including 16 holes (3 cm in diameter arranged in a 4 × 4 pattern) and transparent walls. Mice were allowed to move and explore the holes freely for 20 min. The movements were recorded in a way to be able to observe the head-bobbing behavior at the bottom-up view. The frequency of head bobbing into a hole was counted manually in a blinded manner.

Open-field test. Mice were placed in the center of a white acrylic open-field box (40 × 40 × 40 cm) and allowed to explore freely for 60 min under a complete darkness (0 lux) condition. The size of the center zone was 20 × 20 cm. Locomotion of each mouse was recorded from an infrared camera above and analyzed using EthoVision XT 10 software (Noldus, RRID:SCR_000441).

Elevated plus maze test. The plus maze was made of gray acrylic plates and elevated to a height of 75 cm from the floor with two open arms (30 × 5 × 0.5 cm) and two closed arms (30 × 5 × 30 cm). Light conditions for the open and closed arms were ~250 and ~20 lux, respectively. In the test, mice were introduced to the center of the elevated plus maze and allowed to explore for 8 min. Time spent in open or closed arms was measured using Ethovision XT 10 software (Noldus, RRID:SCR_000441).

Light–dark test. The apparatus consists of dark and light compartments (20 × 30 × 20 cm, 600 lux at light chamber, 20 × 13 × 20 cm, 5 lux at dark chamber), which has a wide entrance between the two chambers (5 cm). Mice were placed in the light chamber with their heads toward to the opposite wall from the dark chamber and allowed to explore the apparatus freely for 10 min. Time spent in light and dark compartment and the number of transitions into the light compartment were analyzed using Ethovision XT 10 software (Noldus, RRID:SCR_000441).

LABORAS test for long-term measurements of movements. Mice were individually caged in an automated system for long-term measurements of rodent behaviors from the start of night cycle (13:00) for 96 or 48 h and fed *ad libitum*. Locomotion, climbing, rearing, grooming, eating, and drinking activities were recorded and automatically analyzed by the LABORAS test (Metris). We did not validate the LABORAS results by manual analyses, based on the previous report that validated LABORAS results (Van de Weerd et al., 2001; Quinn et al., 2003, 2006; Dere et al., 2015).

Electrophysiology. For hippocampal/striatum electrophysiological experiments, mice brains were sectioned in ice-cold dissection buffer containing the following (in mM): 212 sucrose, 25 NaHCO3, 10 D-glucose, 2 Na-pyruvate, 1.25 ascorbic acid, 1.25 NaH_2PO_4, 5 KCl, 3.5 $MgSO_4$, and 0.5 $CaCl_2$ bubbled with 95% O_2/5% CO_2 gas using a Leica VT 1200 vibratome. Brain sections with a thickness of 300 μm were used for whole-cell recordings and thicknesses of 400 μm were used for extracellular field recordings. The slices were recovered for 30 min in artificial CSF (ACSF) at 32°C containing the following (in mM): 124 NaCl, 25 NaHCO3, 10 glucose, 2.5 KCl, 1 NaH_2PO_4, 2 $CaCl_2$, and 2 $MgSO_4$ oxygenated with 95% O_2 5% CO_2 gas. All recordings were performed after recovery for additional 30 min at room temperature. During all recordings, brain slices were maintained in a submerged-type recording chamber perfused with 28°C ACSF (2 ml min^{-1}). Recording and stimulus glass pipettes from borosilicate glass capillaries (Harvard Apparatus) were pulled using an electrode puller (Narishige). All electric responses were amplified and filtered at 2 kHz (Multiclamp 700B; Molecular Devices) and then digitized at 10 kHz (Digidata 1550; Molecular Devices).

For whole-cell patch recordings in the CA1 region of the hippocampus and the dorsolateral region of the striatum, a recording pipette (2.8–3.8 MΩ) was filled with internal solution containing the following (in mM): 100 $CsMeSO_4$, 10 TEA-Cl, 8 NaCl, 10 HEPES, 5 QX-314-Cl, 2 Mg-ATP, 0.3 Na-GTP and 10 EGTA for miniature EPSCs (mEPSCs); 115 CsCl, 10 EGTA, 8 NaCl, 10 TEACl, 10 HEPES, 4 Mg-ATP, 0.3 Na-GTP, and 5 QX-314 for miniature IPSCs (mIPSCs) adjusted to pH 7.35 and 285 mOsm. Medium spiny neurons (MSNs) in the dorsal striatum were identified by the soma size (8–12 μm) and basic membrane properties (cell capacitance > 100 pF and input resistance > 160 MΩ, as described previously (Cepeda et al., 1998, 2008; Gertler et al., 2008). To measure mEPSCs and mIPSCs, CA1 pyramidal neurons and dorsolateral striatal neurons were voltage clamped at −70 mV. For mEPSCs and mIPSCs, picrotoxin (60 μM) and NBQX (10 μM) plus APV (50 μM) were added to ACSF with TTX (1 μM), respectively. For spontaneous EPSCs and IPSCs, picrotoxin (60 μM) and NBQX (10 μM) plus APV (50 μM) without TTX were added, respectively. Responses were recorded for 2 min after maintaining stable baseline for 5 min.

For extracellular field recordings, a stimulating (0.3–0.5 MΩ) and a recording (1 MΩ) pipette were filled with ACSF. Field excitatory postsynaptic potentials (fEPSPs) in the CA1 of the hippocampus were recorded in the stratum radiatum region of the CA1 subfield and the Schaffer collateral pathway in the hippocampus was stimulated. The paired-pulse ratio was measured at intervals of 25, 50, 75, 100, 200, and 300 ms and was defined as the ratio of the mean rise slope of the second fEPSP over that of the first fEPSP.

Brain regional samples and total lysates. Adult *CaMKIIα/Viaat-Cre; Shank2*$^{fl/fl}$ mice and their WT controls were anesthetized with isoflurane and decapitated. The isolated brains were dissected on ice into the following regions: cortex, striatum, hippocampus, and cerebellum. Each brain region was collected and acutely homogenized with ice-cold brain homogenization buffer containing 0.32 M sucrose, 10 mM HEPES, pH 7.4, 2 mM EDTA, 2 mM EGTA, protease inhibitors, and phosphatase inhibitors. Total lysates were prepared by boiling the homogenates with β-mercaptoethanol.

Experimental design and statistical analysis. Statistical analyses were performed using GraphPad Prism 7 software (RRID:SCR_002798). Briefly, the normality of the data distribution was determined using D'Agostino and Pearson omnibus normality test ($n = 8$ or greater) or Kolmogorov–Smirnov normality test ($n < 8$), followed by Student's t test (in the case of normal distribution), Wilcoxon matched-pairs signed rank test, or Mann–Whitney U test (in the case of non-normal distribution). Two-way ANOVA (repeated-measures) and subsequent Bonferroni *post hoc* comparison were used for the analysis of open-field activities and long-term behaviors. Pearson's and Spearman's correlations, for normally and non-normally distributed data, respectively, were used for the analysis of the duration of direct male–female social inter-

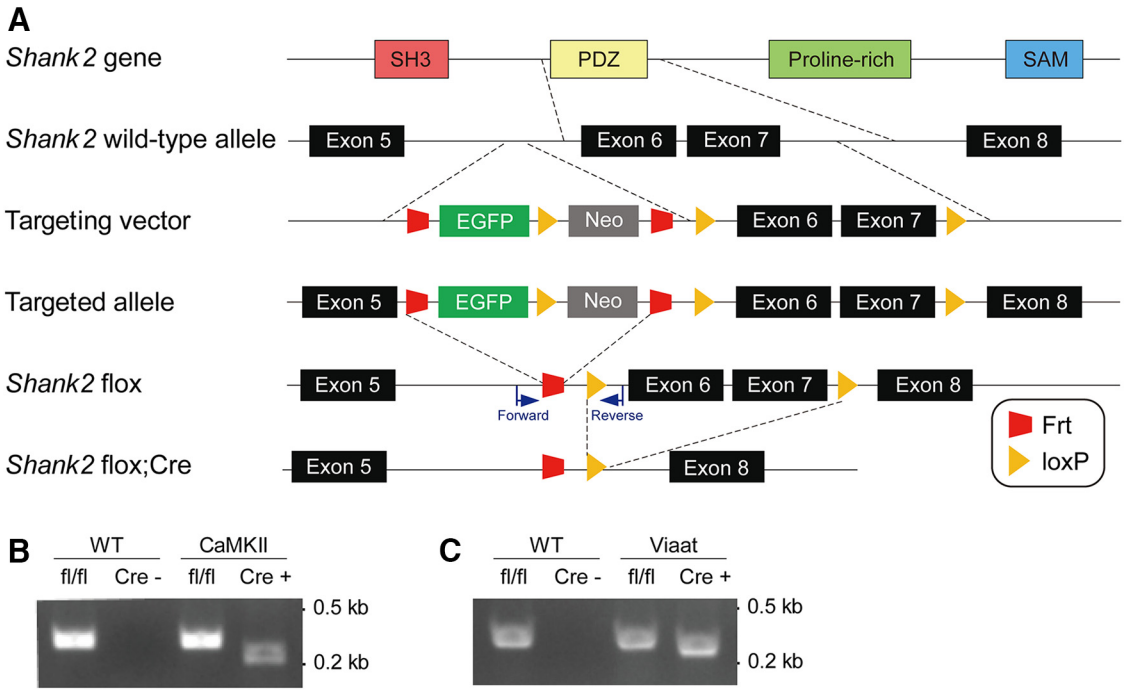

Figure 1. Generation of *CaMKII-Cre;Shank2*$^{fl/fl}$ *and Viaat-Cre;Shank2*$^{fl/fl}$ mice. ***A***, Schematic depiction of the generation of *Shank2* cKO mouse lines. Note that exons 6 and 7 of the *Shank2* gene were targeted. Primer locations for the fl/fl allele are indicated. ***B***, PCR genotyping of *CaMKII-Cre;Shank2*$^{fl/fl}$ mice. WT, *Shank2*$^{fl/fl}$ mice without Cre; CaMKII, *Shank2*$^{fl/fl}$ mice with CaMKII-Cre (*CaMKII-Cre;Shank2*$^{fl/fl}$ mice). ***C***, PCR genotyping of *Viaat-Cre;Shank2*$^{fl/fl}$ mice. WT, *Shank2*$^{fl/fl}$ mice without Cre; Viaat, *Shank2*$^{fl/fl}$ mice with Viaat-Cre (*Viaat-Cre;Shank2*$^{fl/fl}$ mice).

action and the number of USVs during male–female interaction. Sample size was determined based on our previous *Shank2*$^{-/-}$ mice (Won et al., 2012). Details on mice and statistical results can be found in Figure 2-1 (available at https://doi.org/10.1523/JNEUROSCI.2684-17.2018.f2-1) and figure legends.

Results

Generation and characterization of *CaMKII-Cre;Shank2*$^{fl/fl}$ mice

We first generated transgenic mice with a *Shank2* deletion restricted to excitatory neurons (termed *CaMKII-Cre;Shank2*$^{fl/fl}$ mice) by crossing *Shank2*$^{fl/fl}$ mice (exons 6 and 7 floxed; Ha et al., 2016) with *CaMKIIα-Cre* mice (Fig. 1*A*,*B*; also see Materials and Methods for mouse-crossing details; Tsien et al., 1996). An examination of Shank2 protein expression in different brain regions of *CaMKII-Cre;Shank2*$^{fl/fl}$ mice by immunoblotting revealed strong reductions in the levels of Shank2 in the cortex and hippocampus, whereas other brain regions displayed minimal reductions compared with *Shank2*$^{fl/fl}$ mice (referred to WT mice below; Fig. 2*A*; $t_{(4)} = 9.724$, $p = 0.0006$ for Ctx; $t_{(4)} = 0.1982$, $p = 0.8526$ for Str; $t_{(4)} = 2.906$, $p = 0.0438$ for Hp; $t_{(4)} = 0.9001$, $p = 0.4190$ for Cb, one-sample *t* test for all). Levels of Shank1 and Shank3 proteins were not changed in these brain regions of *CaMKII-Cre;Shank2*$^{fl/fl}$ mice (Fig. 2*B*; $t_{(4)} = 0.6556$, $p = 0.5479$ for Ctx Shank1; $t_{(4)} = 0.4664$, $p = 0.6652$ for Ctx Shank3; $t_{(4)} = 0.5315$, $p = 0.6232$ for Str Shank1; $t_{(4)} = 0.9365$, $p = 0.4181$ for Str Shank3; $t_{(4)} = 0.8839$, $p = 0.4267$ for Hp Shank1; $t_{(4)} = 1.636$, $p = 0.1771$ for Hp Shank3; $t_{(4)} = 0.3008$, $p = 0.7832$ for Cb Shank1; $t_{(4)} = 0.3147$, $p = 0.7736$ for Cb Shank3, one sample *t* test for all). Decreased Shank2 expression was further supported by immunofluorescence staining, which showed substantial reductions in Shank2 punctate signals, likely representing their excitatory synaptic localizations (Boeckers et al., 1999b; Tao-Cheng et al., 2015; Heise et al., 2016), in the cortex and CA1 region of the hippocampus (Fig. 2*C*,*D*).

Suppressed excitatory synaptic transmission in *CaMKII-Cre;Shank2*$^{fl/fl}$ mice

Given that Shank2 has been implicated in excitatory synapse development and functional coordination (Boeckers et al., 1999b; Heise et al., 2016), we examined spontaneous excitatory synaptic transmission in hippocampal CA1 pyramidal neurons of *CaMKII-Cre;Shank2*$^{fl/fl}$ mice. We found that the frequency ($t_{(35)} = 3.607$, $p = 0.0010$, unpaired *t* test), but not amplitude ($t_{(35)} = 1.036$, $p = 0.3072$, unpaired *t* test), of mEPSCs was reduced in *CaMKII-Cre;Shank2*$^{fl/fl}$ mice relative to WT (*Shank2*$^{fl/fl}$) mice (Fig. 3*A*). In contrast, mIPSCs were unaffected (Fig. 3*B*; $U = 77.00$, $p = 0.9783$, Mann–Whitney *U* test for frequency; $t_{(23)} = 0.3594$, $p = 0.7226$, unpaired *t* test for amplitude). These results, together with normal paired-pulse facilitation at Schaffer collateral–CA1 synapses (Fig. 3*C*; interaction, $F_{(5,96)} = 0.5$, $p = 0.7754$, genotype, $F_{(1,96)} = 4.25$, $p = 0.0419$, IPIs, $F_{(5,96)} = 22.86$, $p < 0.0001$, repeated-measures two-way ANOVA), suggest that Shank2 expressed in excitatory neurons is important for normal excitatory synaptic transmission in CA1 pyramidal neurons.

CaMKII-Cre;Shank2$^{fl/fl}$ mice show reduced three-chamber and direct social interaction

We next examined behavioral phenotypes in *CaMKII-Cre;Shank2*$^{fl/fl}$ mice. These mice displayed a significantly reduced social approach in the three-chamber test (Silverman et al., 2010), as shown by time spent in sniffing ($t_{(12)} = 7.793$, $p < 0.0001$, paired *t* test for WT; $W = 69.00$, $p = 0.0134$, Wilcoxon matched-pairs signed-rank test for cKO) and a preference index (see figure legends for details; $t_{(24)} = 3.668$, $p = 0.0008$, unpaired *t* test; Fig. 4*A*). In contrast, social novelty recognition was normal in these mice (Fig. 4*B*; $t_{(12)} = 4.027$, $p = 0.0017$, paired *t* test for time spent in sniffing in WT; $t_{(12)} = 3.241$, $p = 0.0071$, paired *t* test for time spent in sniffing in cKO; $t_{(24)} = 0.9204$, $p = 0.3665$, unpaired *t* test for preference index). These results are similar to the re-

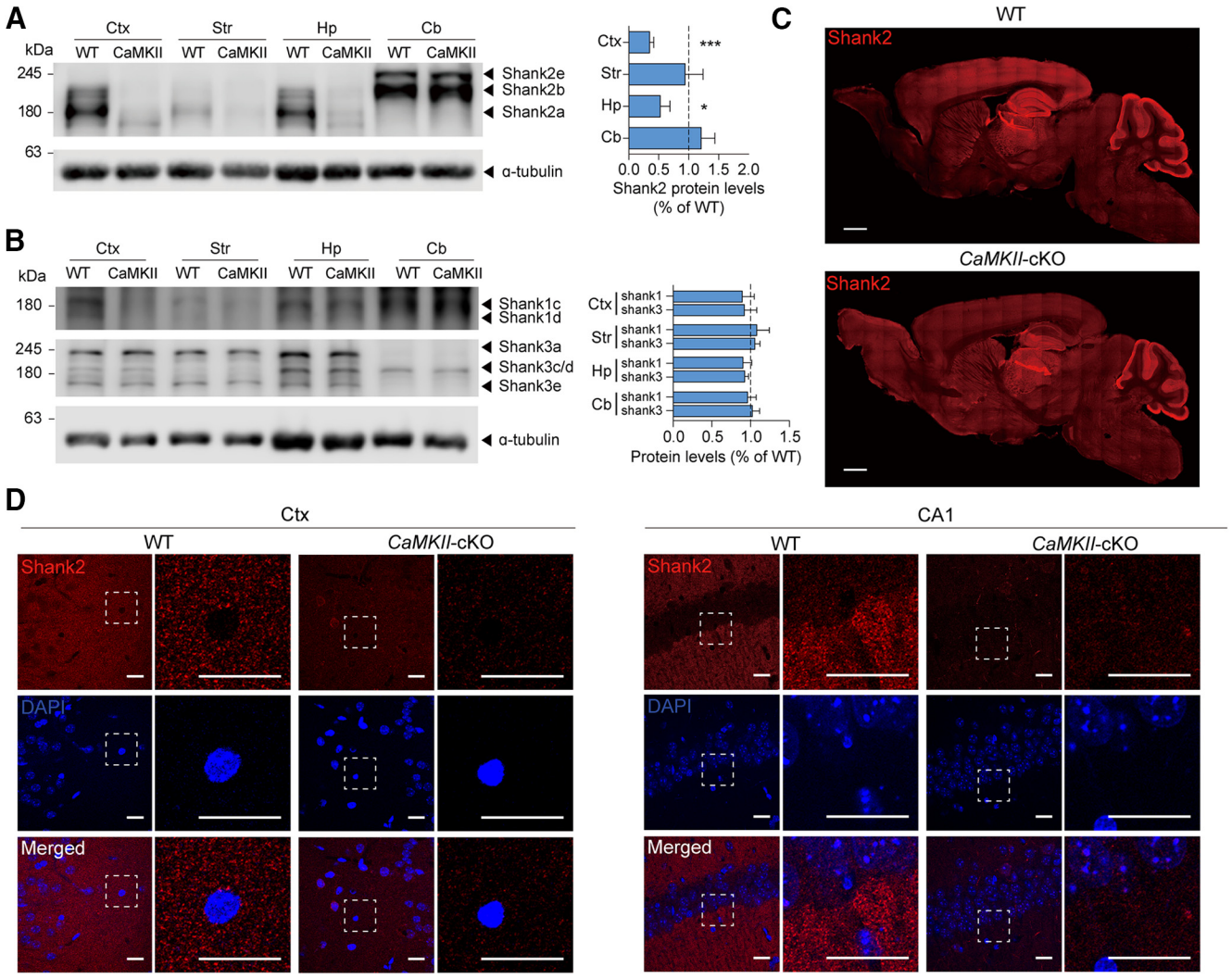

Figure 2. Characterization of Shank2 protein expression in *CaMKII-Cre;Shank2*$^{fl/fl}$ mice. ***A***, Shank2 protein expression in different brain regions of *CaMKII-Cre;Shank2*$^{fl/fl}$ mice (12 weeks), revealed by immunoblot analysis of total lysates. Ctx, Cortex; Str, striatum; Hp, hippocampus; Cb, cerebellum. Shank2 protein levels in *CaMKII-Cre;Shank2*$^{fl/fl}$ mice were normalized to those from WT mice. The indicated specific Shank2 splice variants are based on previous reports (Schmeisser et al., 2012; Won et al., 2012). Data are shown as mean ± SEM. $n = 5$ mice for WT and cKO, $^{*}p < 0.05$, $^{***}p < 0.001$, one-sample *t* test (see Fig. 2-1, available at https://doi.org/10.1523/JNEUROSCI.2684-17.2018.f2-1, for additional details). ***B***, Levels of Shank1 and Shank3 proteins in different brain regions of *CaMKII-Cre;Shank2*$^{fl/fl}$ mice (12 weeks), revealed by immunoblot analysis of total lysates. Shank1 and Shank3 protein levels in *CaMKII-Cre;Shank2*$^{fl/fl}$ mice were normalized to those from WT mice. The indicated specific Shank1/3 splice variants are based on previous reports (Lim et al., 1999; Wang et al., 2014b). $n = 5$ mice for WT and cKO, one-sample *t* test. ***C***, Shank2 protein expression in different brain regions of *CaMKII-Cre;Shank2*$^{fl/fl}$ mice (6 months), as revealed by immunofluorescence staining for Shank2. Scale bar, 1 mm. ***D***, Reduced Shank2 protein levels in the *CaMKII-Cre;Shank2*$^{fl/fl}$ cortex (Ctx) and hippocampal CA1 regions (3 months). DAPI was used for nuclear staining. Scale bar, 20 μm.

duced social interaction and normal social novelty recognition observed in conventional *Shank2*$^{-/-}$ mice (exons 6 and 7; Won et al., 2012).

In a test for social communication based on USVs, *CaMKII-Cre;Shank2*$^{fl/fl}$ mice emitted normal numbers of USVs ($U = 103.5$, $p = 0.4025$ for number of USV during baseline periods; $U = 91.5$, $p = 0.1964$ for number of USV during test periods, Mann–Whitney *U* test for all), but showed significantly increased latency to emit the first USV (Fig. 4*C*; $U = 62$, $p = 0.0159$, Mann–Whitney *U* test). These results are partly similar to the reduced USV number and increased latency to first USV observed in conventional *Shank2*$^{-/-}$ mice (exons 6 and 7; Won et al., 2012). In addition, *CaMKII-Cre;Shank2*$^{fl/fl}$ mice showed reduced levels of male–female social interaction under this context, as measured by the total time spent sniffing, following, and mounting, which positively correlated with the number of USVs (Fig. 4*C*; $U = 69$, $p = 0.0319$, Mann–Whitney *U* test for interaction time; $r = 0.6845$, $p < 0.0001$, Spearman's correlation for correlational analysis of interaction time and number of calls).

In tests for repetitive behaviors, *CaMKII-Cre;Shank2*$^{fl/fl}$ mice showed normal self-grooming ($U = 130.0$, $p = 0.4765$, Mann–Whitney *U* test) and jumping behavior ($U = 128.0$, $p = 0.3579$, Mann–Whitney *U* test), but reduced digging ($t_{(33)} = 3.826$, $p = 0.0005$, unpaired *t* test) in their home cages (Fig. 4*D*). *CaMKII-Cre;Shank2*$^{fl/fl}$ mice also showed normal self-grooming in the LABORAS test, in which mouse movements were monitored continuously for 96 h (Fig. 4*E*; interaction, $F_{(95, 1710)} = 1.22$, $p = 0.0760$; genotype, $F_{(1,18)} = 1.21$, $p = 0.2857$; time, $F_{(95,1710)} = 5.11$, $p < 0.0001$, repeated-measures two-way ANOVA for 1 h binned grooming duration; $U = 46.0$, $p = 0.7959$, Mann–Whitney *U* test for total grooming duration), similar to the normal self-grooming of conventional *Shank2*$^{-/-}$ mice in LABORAS cages, an experiment performed for comparison (Fig. 4*F*; inter-

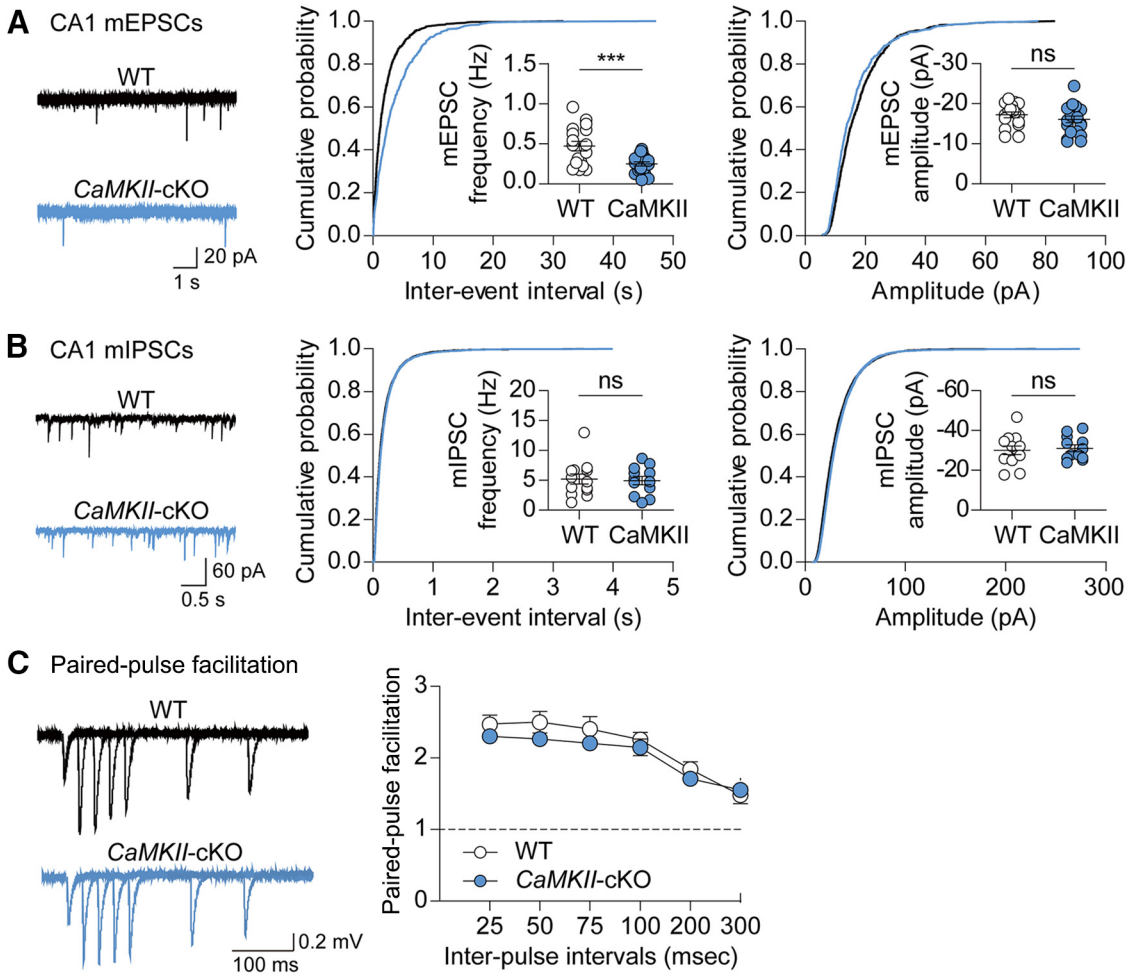

Figure 3. Excitatory and inhibitory synaptic transmission in the CA1 region of the *CaMKII-Cre;Shank2*$^{fl/fl}$ hippocampus. ***A***, ***B***, Reduced frequency but normal amplitude of mEPSCs (***A***) and normal frequency and amplitude of mIPSCs (***B***) in CA1 pyramidal neurons of the *CaMKII-Cre;Shank2*$^{fl/fl}$ hippocampus (P22–P26). $n = 17$ cells from 4 mice for WT; $n = 20$ cells from 5 mice for cKO for mEPSCs, and $n = 13$ cells from 3 mice for WT and $n = 12$ from 3 mice for cKO for mIPSCs. ***$p < 0.001$, ns (not significant), Mann–Whitney *U* test and Student's *t* test. ***C***, Normal levels of paired-pulse facilitation at Schaffer collateral–CA1 pyramidal cell synapses in the *CaMKII-Cre;Shank2*$^{fl/fl}$ hippocampus (P22–P26), as indicated by the slopes of fEPSPs plotted against interpulse intervals. $n = 9$ slices from 3 mice for WT and cKO, two-way ANOVA.

action, $F_{(47,517)} = 1.65$, $p = 0.0055$; genotype, $F_{(1,11)} = 0$, $p = 0.9557$; time, $F_{(47,517)} = 2.64$, $p < 0.0001$, repeated-measures two-way ANOVA for 1 h binned grooming duration; $t_{(11)} = 0.05678$, $p = 0.9557$, unpaired *t* test for total grooming duration). In the hole-board test, another test for repetitive behavior, *CaMKII-Cre;Shank2*$^{fl/fl}$ mice displayed normal levels of head bobbing (Fig. 4*G*; $t_{(24)} = 0.4989$, $p = 0.6224$, unpaired *t* test). These results suggest that, apart from a reduction in digging behavior, *Shank2* deletion in excitatory neurons has small effects on repetitive behaviors in mice and that *CaMKII-Cre;Shank2*$^{fl/fl}$ mice and conventional *Shank2*$^{-/-}$ mice show similar repetitive behaviors such as normal self-grooming and reduced digging, although jumping is increased only in conventional *Shank2*$^{-/-}$ mice (Won et al., 2012).

CaMKII-Cre;Shank2$^{fl/fl}$ mice show mild hyperactivity and anxiety-like behaviors

Conventional *Shank2*$^{-/-}$ mice display severe hyperactivity in the open-field arena (~2-fold increase in total distance moved) under dim light conditions (<10 lux; Won et al., 2012). *CaMKII-Cre;Shank2*$^{fl/fl}$ mice subjected to the open-field test, corresponding to a novel environment, displayed mild hyperactivity (~17% increase) in complete darkness (0 lux; Fig. 5*A*; interaction, $F_{(5,130)} = 0.49$, $p = 0.7805$; genotype, $F_{(1,26)} = 4.83$, $p = 0.0371$; time, $F_{(5,130)} = 65.63$, $p < 0.0001$, repeated-measures two-way ANOVA for 1 h binned distance moved; $t_{(26)} = 2.198$, $p = 0.0371$, unpaired *t* test for total distance moved). In the LABORAS test, *CaMKII-Cre;Shank2*$^{fl/fl}$ mice displayed hyperactivity during the first 12 h beginning after a few hours in the chamber, but this behavior did not persist into the following days and did not lead to a significant change in the total distance moved (Fig. 5*B*; interaction, $F_{(95, 1710)} = 1.88$, $p < 0.0001$; genotype, $F_{(1,18)} = 1.94$, $p = 0.1807$; time, $F_{(95,1710)} = 9.09$, $p < 0.0001$, repeated-measures two-way ANOVA for 1 h binned distance moved; $t_{(18)} = 1.349$, $p = 0.1942$, unpaired *t* test for first 6 h; $U = 10.00$, $p = 0.0015$ for first 12 h; $U = 34.00$, $p = 0.2475$ for total distance moved, Mann–Whitney *U* test for both). In contrast, conventional *Shank2*$^{-/-}$ mice showed strong hyperactivity in LABORAS cages (Fig. 5*C*; interaction, $F_{(47,517)} = 2.95$, $p < 0.0001$; genotype, $F_{(1,11)} = 7.47$, $p = 0.0195$; time, $F_{(47,517)} = 12.55$, $p < 0.0001$, repeated-measures two-way ANOVA for 1 h binned distance moved; $t_{(11)} = 2.720$, $p = 0.0199$, unpaired *t* test for first 6 h; $t_{(11)} = 2.733$, $p = 0.0195$, unpaired *t* test for total distance moved). These results suggest that *CaMKII-Cre;Shank2*$^{fl/fl}$ mice show mild hyperactivity somewhat similar to the strong hyperactivity of conventional *Shank2*$^{-/-}$ mice.

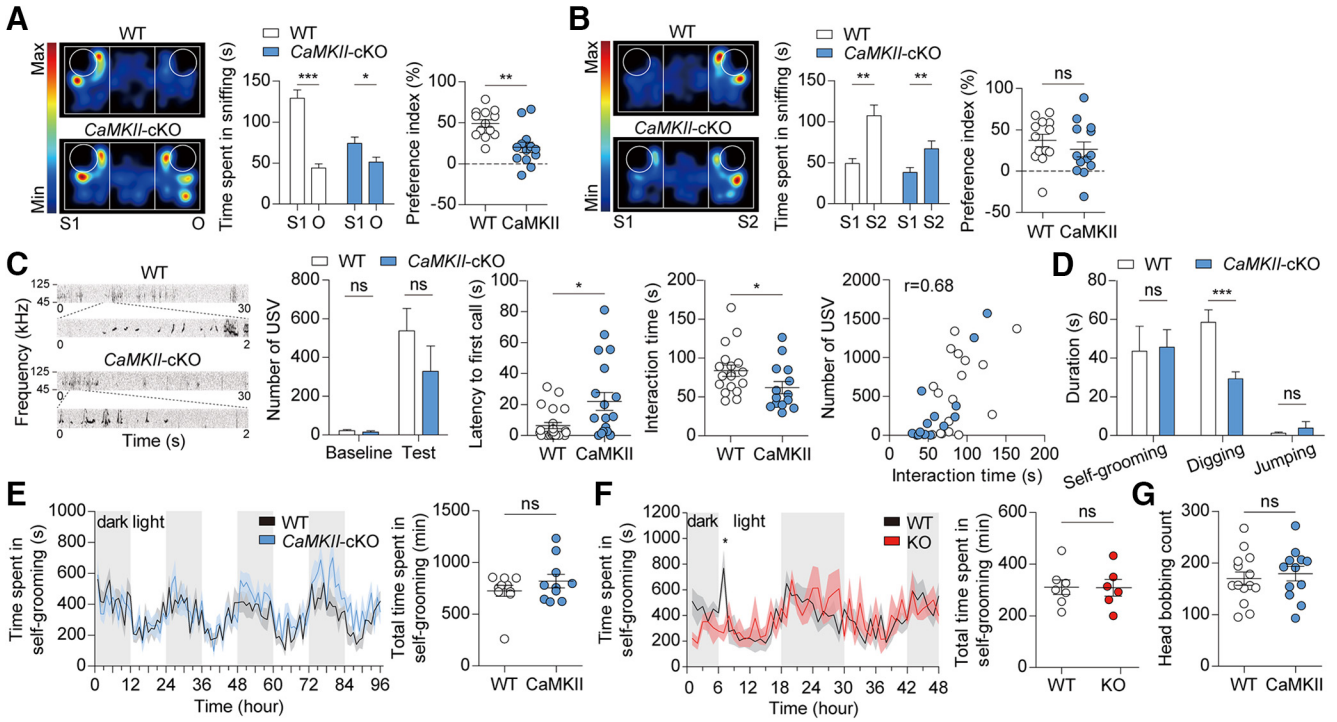

Figure 4. *CaMKII-Cre;Shank2*$^{fl/fl}$ mice show reduced three-chamber and direct social interactions. ***A***, ***B***, Reduced social approach (***A***), but normal social novelty recognition (***B***) in *CaMKII-Cre;Shank2*$^{fl/fl}$ mice (9–12 weeks; males) in the three-chamber social interaction test, as shown by time spent sniffing a target (S1, O, or S2) and the social preference index (S1-O [or S2–S1]/the sum of the two parameters × 100). Data are shown as mean ± SEM. $n = 13$ mice for WT and cKO, $^*p < 0.05$, $^{**}p < 0.01$, $^{***}p < 0.001$, ns, not significant, Wilcoxon matched-pairs signed-rank test (for time in sniffing in cKO) and Student's *t* test (for time in sniffing in WT and preference index). ***C***, Normal numbers of USVs (basal and female encounter), but increased time to emit the first USV, in *CaMKII-Cre;Shank2*$^{fl/fl}$ mice (9–12 weeks). Note that direct male–female social interaction was reduced, as measured by the time spent in sniffing, following, and mounting in males, which shows a positive correlation with the number of USVs ($r = 0.68$, $n = 32$, 18 for WT and 14 for cKO combined, Spearman's correlation). $n = 18$ mice for WT and 14 for cKO, $^*p < 0.05$, ns, not significant, Mann–Whitney *U* test. ***D***, Normal self-grooming and jumping but reduced digging in *CaMKII-Cre;Shank2*$^{fl/fl}$ mice (10–13 weeks) in home cages. $n = 19$ mice for WT and 16 for cKO, $^{***}p < 0.001$, ns (not significant), Mann–Whitney *U* test and Student's *t* test (for digging). ***E***, Normal self-grooming in *CaMKII-Cre;Shank2*$^{fl/fl}$ mice (13–17 weeks) in the LABORAS test, in which mouse movements are monitored continuously for 96 h. $n = 10$ mice for WT and cKO, ns (not significant), two-way ANOVA and Mann–Whitney *U* test. ***F***, Normal self-grooming of conventional *Shank2*$^{-/-}$ mice (12–15 weeks) in the LABORAS test performed for comparative purposes. Data are shown as mean ± SEM. $n = 7$ mice for WT and 6 for KO (*Shank2*$^{-/-}$), $^*p < 0.05$, ns (not significant), two-way ANOVA and Student's *t* test. ***G***, Normal head bobbing of *CaMKII-Cre;Shank2*$^{fl/fl}$ mice (10–13 weeks) in the hole-board test. $n = 14$ mice for WT and 12 for cKO, ns (not significant), Student's *t* test.

Conventional *Shank2*$^{-/-}$ mice show anxiety-like behavior in the elevated plus maze, but not in the open-field test or light–dark apparatus (Won et al., 2012). *CaMKII-Cre;Shank2*$^{fl/fl}$ mice showed anxiety-like behavior in an open-field arena (reduced center time; $t_{(26)} = 2.438$, $p = 0.0219$, unpaired *t* test) and in a light–dark chamber ($U = 25.00$, $p = 0.0229$, Mann–Whitney *U* test for time in light chamber; $t_{(20)} = 1.308$, $p = 0.2059$, unpaired *t* test for number of transition), but not in an elevated plus maze ($t_{(20)} = 1.145$, $p = 0.2657$ for time in open arms; $t_{(20)} = 1.341$, $p = 0.1950$ for time in closed arms, unpaired *t* test for all; Fig. 5*D*,*E*), a pattern complementary to that of conventional *Shank2*$^{-/-}$ mice. These results suggest that *Shank2*$^{-/-}$ and *CaMKII-Cre;Shank2*$^{fl/fl}$ mice show mild but distinct anxiety-like behaviors.

The observed behavioral abnormalities in *CaMKII-Cre;Shank2*$^{fl/fl}$ mice might be attributable to the inherent phenotypes in *CaMKII-Cre* mice. To address this possibility, we subjected *CaMKII-Cre* mice to a series of behavioral tests in which *CaMKII-Cre;Shank2*$^{fl/fl}$ mice showed positive behavioral alterations. *CaMKII-Cre* mice showed normal levels of social interaction (3-chamber; $t_{(7)} = 5.643$, $p = 0.0008$, paired *t* test for time spent in sniffing in WT; $t_{(7)} = 15.76$, $p < 0.0001$, paired *t* test for time spent in sniffing in Cre; $t_{(14)} = 1.287$, $p = 0.2189$, unpaired *t* test for preference index), repetitive digging ($t_{(22)} = 0.1533$, $p = 0.8795$, unpaired *t* test), USVs ($t_{(16)} = 1.210$, $p = 0.2440$, for number of USV during baseline periods and $t_{(16)} = 0.1579$, $p = 0.8765$, for number of USVs during test periods, unpaired *t* test for both; $U = 24.00$, $p = 0.1615$, Mann–Whitney *U* test for latency to the first call), social interaction during USV ($t_{(16)} = 0.4309$, $p = 0.6723$, unpaired *t* test for interaction time; $r = 0.5998$, $p = 0.0085$, Pearson's correlation for correlational analysis of interaction time and number of calls), locomotor activity (open-field: interaction, $F_{(5,70)} = 0.25$, $p = 0.9389$; genotype, $F_{(1,14)} = 0.22$, $p = 0.6487$; time, $F_{(5,70)} = 45.62$, $p < 0.0001$, repeated-measures two-way ANOVA for 1 h binned distance moved; $t_{(14)} = 0.4656$, $p = 0.6486$, unpaired *t* test for total distance moved; $U = 31.00$, $p = 0.9591$, Mann–Whitney *U* test for time in center) and LABORAS (interaction, $F_{(95,1235)} = 0.99$, $p = 0.4969$; genotype, $F_{(1,13)} = 2.05$, $p = 0.1755$; time, $F_{(95,1235)} = 13.72$, $p < 0.0001$, repeated-measures two-way ANOVA for 1 h binned distance moved; $t_{(13)} = 1.373$, $p = 0.1930$, unpaired *t* test for first 6 h, $t_{(13)} = 1.084$, $p = 0.2978$, unpaired *t* test for 12 h; $U = 15.00$, $p = 0.1520$, Mann–Whitney *U* test for total distance moved), and anxiety-like behavior (light–dark; $U = 18.00$, $p = 0.1605$, Mann–Whitney *U* test for time in light chamber; $t_{(14)} = 0.3441$, $p = 0.7359$, unpaired *t* test for number of transition; Fig. 6*A*–*F*).

Generation and characterization of *Viaat-Cre;Shank2*$^{fl/fl}$ mice

The results described thus far were from mice lacking Shank2 protein in excitatory neurons. To investigate the effects of *Shank2* deletion in GABAergic inhibitory neurons, we crossed *Shank2*$^{fl/fl}$

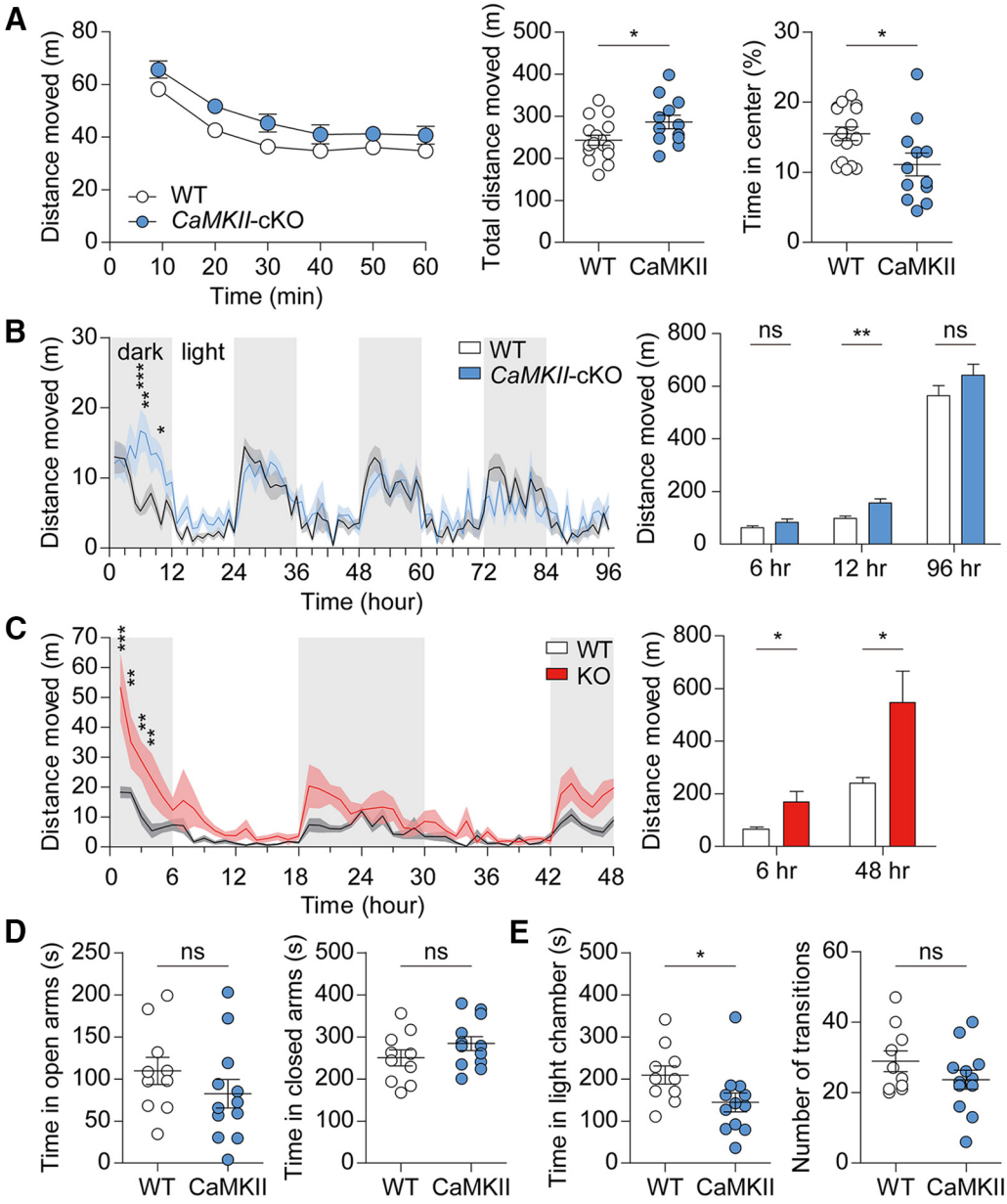

Figure 5. *CaMKII-Cre;Shank2*$^{fl/fl}$ mice show mild hyperactivity and anxiety-like behaviors. ***A***, Mild hyperactivity of *CaMKII-Cre;Shank2*$^{fl/fl}$ mice (9–12 weeks) in the open-field test (a novel environment) under a complete darkness (0 lux) condition. Note that these mice show anxiety-like behavior, as evidenced by the decreased time spent in the center region of the open-field arena. Data are shown as mean ± SEM. $n = 16$ for WT and 12 for cKO, $^*p < 0.05$, two-way ANOVA and Student's *t* test. ***B***, Mild hyperactivity of *CaMKII-Cre;Shank2*$^{fl/fl}$ mice (13–17 weeks) in the LABORAS test (a familiar environment), in which mouse movements are monitored continuously for 96 h. Note that *CaMKII-Cre;Shank2*$^{fl/fl}$ mice are hyperactive during the first 12 h, but not throughout the entire 96 h monitoring period. $n = 10$ mice for WT and cKO, $^*p < 0.05$, $^{**}p < 0.01$, $^{***}p < 0.001$, ns (not significant), two-way ANOVA and Mann–Whitney *U* test (for first 12 h and total 96 h) and Student's *t* test (for first 6 h). ***C***, Increased locomotor activity of conventional *Shank2*$^{-/-}$ mice (12–15 weeks) in the LABORAS test, a test performed for comparison, as shown by distance moved. Note that the first 6 h, not 12 h, were used for the analysis of early hyperactivity. $n = 7$ mice for WT and 6 for KO, $^*p < 0.05$, $^{**}p < 0.01$, $^{***}p < 0.001$, ns (not significant), two-way ANOVA and Student's *t* test. ***D***, Normal anxiety-like behavior of *CaMKII-Cre;Shank2*$^{fl/fl}$ mice (12–15 weeks) in the elevated plus maze test. $n = 10$ mice for WT and 12 for cKO, ns (not significant), Student's *t* test. ***E***, Anxiety-like behavior of *CaMKII-Cre;Shank2*$^{fl/fl}$ mice (12–16 weeks) in the light–dark test. $n = 10$ mice for WT and 12 for cKO, $^*p < 0.05$, ns (not significant), Student's *t* test and Mann–Whitney *U* test (for time in light chamber).

mice (exons 6 and 7) with *Viaat-Cre* mice, which express Cre globally in GABAergic neurons (Chao et al., 2010), to generate *Viaat-Cre;Shank2*$^{fl/fl}$ mice (Fig. 1*A*,*C*). An examination of the expression levels of Shank2 protein in different brain regions of *Viaat-Cre;Shank2*$^{fl/fl}$ mice by immunoblot analysis revealed marked reductions in the levels of Shank2 in the striatum and cerebellum (Fig. 7*A*; $t_{(4)} = 1.753$, $p = 0.1544$ for Ctx; $t_{(4)} = 21.62$, $p < 0.0001$ for Str; $t_{(3)} = 0.3906$, $p = 0.7222$ for Hp; $t_{(4)} = 109.1$, $p < 0.0001$ for Cb, one-sample *t* test for all), where GABAergic inhibitory neurons are abundant. Levels of Shank1 and Shank3 proteins were not changed in these brain regions of *Viaat-Cre;Shank2*$^{fl/fl}$ mice (Fig. 7*B*; $t_{(4)} = 0.8195$, $p = 0.4585$ for Ctx Shank1; $t_{(4)} = 0.8350$, $p = 0.4650$ for Ctx Shank3; $t_{(4)} = 2.069$, $p = 0.1074$ for Str Shank1; $t_{(4)} = 0.9702$, $p = 0.3869$ for Str Shank3; $t_{(3)} = 0.03027$, $p = 0.9773$ for Hp Shank1; $t_{(3)} = 0.5986$, $p = 0.5916$ for Hp Shank3; $t_{(4)} = 0.1315$, $p = 0.9017$ for Cb Shank1; $t_{(4)} = 1.743$, $p = 0.1563$ for Cb Shank3, one-sample *t* test for all). Immunofluorescence staining of *Viaat-Cre;Shank2*$^{fl/fl}$ slices showed strong reductions in Shank2 signals in the striatum and cerebellum (Fig. 7*C*,*D*).

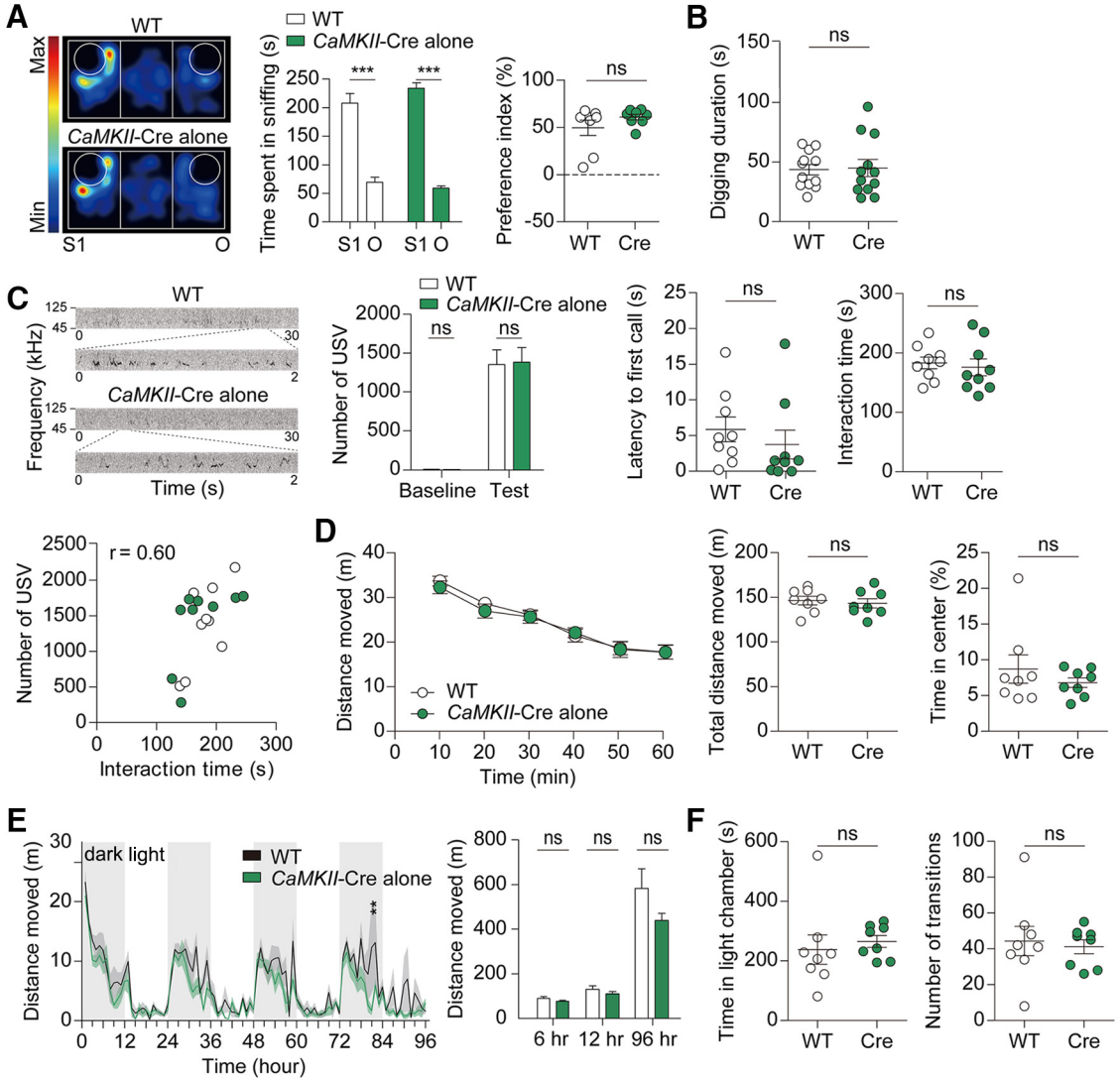

Figure 6. *CaMKII-Cre* mice show normal social interaction, digging, USVs, locomotor activity, and anxiety-like activity. ***A***, Normal social interaction of *CaMKII-Cre* mice (10 weeks) in the three-chamber social interaction test, as shown by time spent sniffing a target (S1, 0, or S2) and the social preference index. $n = 8$ mice for WT and CaMKII-Cre, $^{***}p < 0.001$, ns (not significant), Student's *t* test. ***B***, Normal digging in *CaMKII-Cre* mice (8 weeks), as shown by digging duration. $n = 12$ for WT and CaMKII-Cre, ns (not significant), Student's *t* test. ***C***, Normal numbers of USVs (basal and female encounter) and latency to first call in *CaMKII-Cre* mice (9 weeks; males). Note that direct male–female social interaction is normal *CaMKII-Cre* mice, as measured by the time spent in sniffing, following, and mounting in males, which shows a positive correlation with the number of USVs ($r = 0.60$, $n = 18$, WT and CaMKII-Cre combined, Pearson's correlation). $n = 9$ mice for WT and CaMKII-Cre, ns (not significant), Mann–Whitney *U* test (for latency to first call) and Student's *t* test. ***D***, Normal locomotor activity of *CaMKII-Cre* mice (9 weeks) in the open-field test under 100 lux condition. Note that these mice also show normal anxiety-like behavior, as evidenced by the normal time spent in the center region of the open-field arena. $n = 8$ for WT and CaMKII-Cre, ns (not significant), two-way ANOVA, Student's *t* test, and Mann–Whitney *U* test (for time in center). ***E***, Normal locomotor activity of *CaMKII-Cre* mice (11 weeks) in the LABORAS test, as shown by distance moved. $n = 8$ mice for WT and 7 for CaMKII-Cre, $^{**}p < 0.01$, ns (not significant), two-way ANOVA, Student's *t* test (for 6 and 12 h), and Mann–Whitney *U* test (for 96 h). ***F***, Normal anxiety-like behavior of *CaMKII-Cre* mice (10 weeks) in the light– dark test. $n = 8$ mice for WT and CaMKII-Cre, ns (not significant), Student's *t* test and Mann–Whitney *U* test (for time in light chamber).

Suppressed inhibitory transmission in the *Viaat-Cre;Shank2*$^{fl/fl}$ striatum

To determine whether Shank2 contributes to excitatory synaptic transmission in *Viaat-Cre;Shank2*$^{fl/fl}$ mice, we measured mEPSCs from the neurons in the dorsolateral striatum, a region enriched with GABAergic MSNs. We found that both the frequency ($t_{(27)} = 1.057$, $p = 0.2998$, unpaired *t* test) and amplitude ($t_{(27)} = 0.3796$, $p = 0.7072$, unpaired *t* test) of mEPSCs were normal in *Viaat-Cre;Shank2*$^{fl/fl}$ mice relative to WT mice (Fig. 8*A*). In contrast, both the frequency ($U = 53.00$, $p = 0.0030$, Mann–Whitney *U* test) and amplitude ($U = 77.00$, $p = 0.0351$, Mann–Whitney *U* test) of mIPSCs were reduced in *Viaat-Cre;Shank2*$^{fl/fl}$ mice (Fig. 8*B*), possibly because of defects in neighboring MSNs that provide the majority of inhibitory synaptic inputs (Guzmán et al., 2003).

When spontaneous EPSCs (sEPSCs)/sIPSCs were measured in the same region in the absence of tetrodotoxin to allow action potential firings (Fig. 8*C*,*D*), sIPSC amplitude ($t_{(21)} = 2.362$, $p = 0.0279$, unpaired *t* test), but not frequency ($t_{(21)} = 0.8712$, $p = 0.3935$, unpaired *t* test), was decreased in *Viaat-Cre;Shank2*$^{fl/fl}$ neurons, suggesting that the suppressed mIPSC frequency, but not amplitude, was normalized by network activity. In addition, sEPSC frequency ($t_{(35)} = 2.087$, $p = 0.0442$, unpaired *t* test), but not amplitude ($t_{(35)} = 1.024$, $p = 0.3129$, unpaired *t* test), was decreased, likely to maintain the balance of synaptic excitation and inhibition.

In the hippocampal CA1 region, where *Viaat*-specific *Shank2* deletion had minimal effects on total levels of Shank2 protein, *Viaat-Cre;Shank2*$^{fl/fl}$ pyramidal neurons showed normal mEPSCs ($U = 151.0$, $p = 0.9605$, for frequency; $U = 139.0$, $p = 0.6559$ for

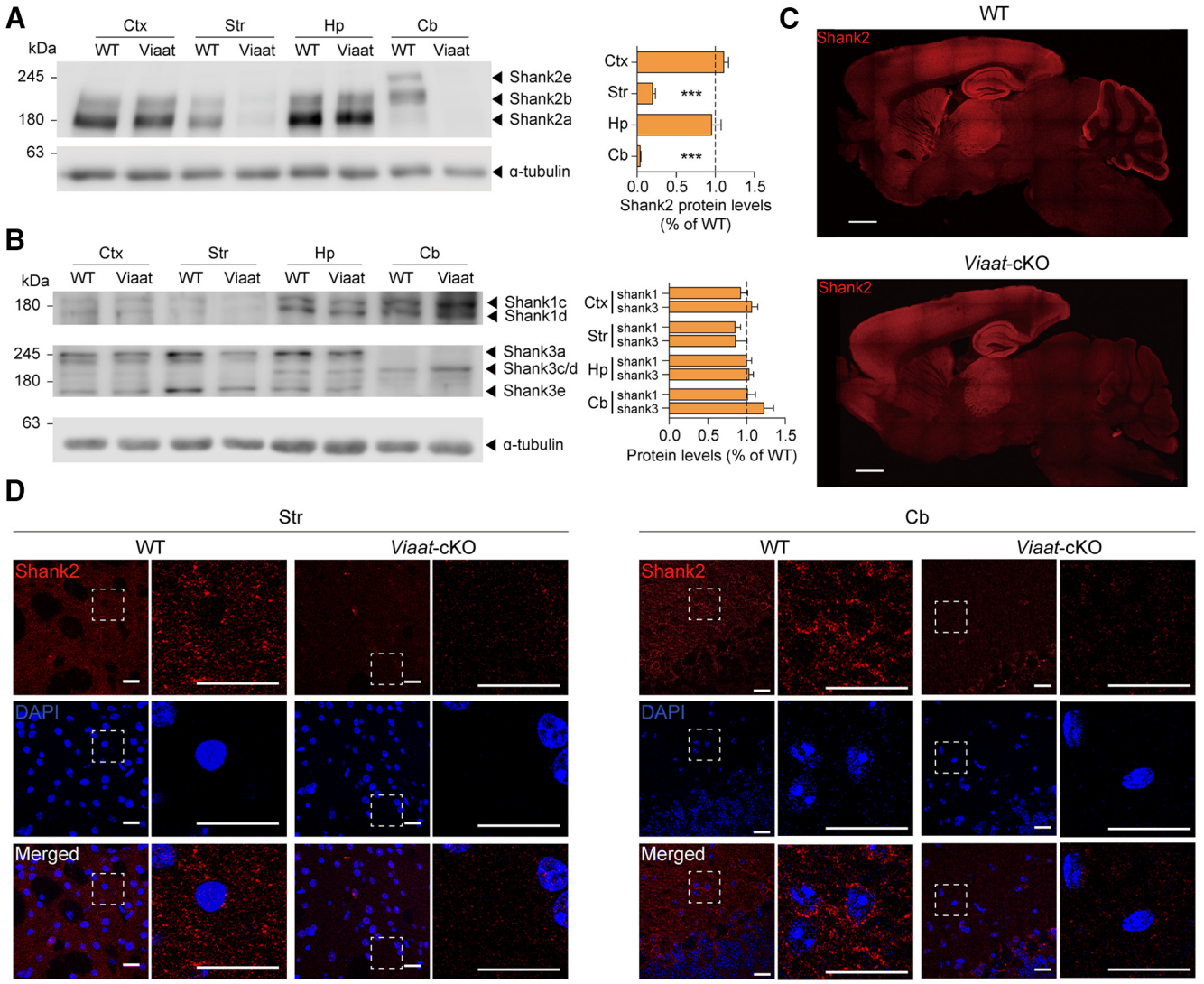

Figure 7. Generation and characterization of *Viaat-Cre;Shank2*$^{fl/fl}$ mice. ***A***, Shank2 protein expression in different brain regions of *Viaat-Cre;Shank2*$^{fl/fl}$ mice (10 weeks) revealed by immunoblot analysis of total lysates. Str, Striatum; Ctx, cortex; Hp, hippocampus; Cb, cerebellum. Shank2 protein levels in *Viaat-Cre;Shank2*$^{fl/fl}$ mice were normalized to those from WT mice. Data are shown as mean ± SEM. $n = 5$ mice for WT and cKO except for the hippocampus (4 mice). ***$p < 0.001$, one-sample t test. ***B***, Normal levels of Shank1 and Shank3 proteins in different brain regions of *Viaat-Cre;Shank2*$^{fl/fl}$ mice (10 weeks) revealed by immunoblot analysis of total lysates. Shank1 and Shank3 protein levels in *Viaat-Cre;Shank2*$^{fl/fl}$ mice were normalized to those from WT mice. The indicated specific Shank1/3 splice variants are based on previous reports (Lim et al., 1999; Wang et al., 2014b). $n = 5$ mice for WT and cKO except for hippocampus ($n = 4$), one-sample t test. ***C***, Shank2 protein expression in different brain regions of *Viaat-Cre;Shank2*$^{fl/fl}$ mice (4 months) revealed by immunofluorescence staining for Shank2. Scale bar, 1 mm. ***D***, Reduced Shank2 protein levels in the striatum (Str) and cerebellum (Cb) of *Viaat-Cre;Shank2*$^{fl/fl}$ mice (4 months). DAPI was used for nuclear staining. Scale bar, 20 μm.

amplitude, Mann–Whitney U test for all) and mIPSCs ($t_{(38)} = 0.7262$, $p = 0.4722$ for frequency; $t_{(38)} = 0.3718$, $p = 0.7121$ for amplitude, unpaired t test for all; Fig. 8*E*,*F*). These results collectively suggest that *Shank2* deletion in GABAergic interneurons has strong influences on inhibitory synaptic transmission in the striatum.

Viaat-Cre;Shank2$^{fl/fl}$ mice show normal three-chamber social interaction, but reduced direct social interaction, reduced USVs, and increased self-grooming

An examination of behavioral phenotypes in *Viaat-Cre;Shank2*$^{fl/fl}$ mice showed normal levels of social approach ($t_{(20)} = 12.23$, $p < 0.0001$, paired t test for time spent in sniffing in WT; $t_{(16)} = 8.240$, $p < 0.0001$, paired t test for time spent in sniffing in cKO; $t_{(36)} = 0.2634$, $p = 0.7938$, unpaired t test for preference index) and social novelty recognition ($t_{(20)} = 4.063$, $p = 0.0006$, paired t test for time spent in sniffing in WT; $t_{(16)} = 3.220$, $p = 0.0054$, paired t test for time spent in sniffing in cKO; $t_{(36)} = 0.009964$, $p = 0.9921$, unpaired t test for preference index) in the three-chamber test (Fig. 9*A*,*B*). *Viaat-Cre;Shank2*$^{fl/fl}$ mice, however, showed markedly reduced numbers of USVs ($U = 138.0$, $p = 0.4082$, for number of calls during baseline periods; $U = 55.00$, $p = 0.0007$, for number of calls during test periods, Mann–Whitney U test for both) and increased time to emit the first USV ($U = 81.00$, $p = 0.0098$, Mann–Whitney U test; Fig. 9*C*). In addition, these mice show reduced direct male–female social interaction under this context ($t_{(35)} = 2.535$, $p = 0.0159$, unpaired t test for interaction time), as measured by the total time spent in sniffing, following, and mounting, a parameter positively correlated with the number of USVs ($r = 0.6608$, $p < 0.0001$, Spearman's correlation; Fig. 9*C*).

We next tested repetitive behaviors in *Viaat-Cre;Shank2*$^{fl/fl}$ mice and found that they displayed enhanced self-grooming in their home cages ($U = 91.5$, $p = 0.0071$, Mann–Whitney U

test), but showed normal digging behaviors ($t_{(37)} = 1.305$, $p = 0.2000$, unpaired t test) and jumping behaviors ($U = 164.0$, $p = 0.2263$, Mann–Whitney U test; Fig. 9*D*). Enhanced self-grooming was also observed in the LABORAS test (Fig. 9*E*; interaction, $F_{(94,3478)} = 1.43$, $p = 0.0044$; genotype, $F_{(1,37)} = 11.76$, $p = 0.0015$; time, $F_{(94,3478)} = 10.76$, $p < 0.0001$, repeated-measures two-way ANOVA for 1 h binned grooming duration; $t_{(37)} = 3.432$, $p = 0.0015$, unpaired t test for total grooming duration). In addition, *Viaat-Cre;Shank2*$^{fl/fl}$ mice displayed enhanced head bobbing in the hole-board test (Fig. 9*F*; $t_{(38)} = 4.991$, $p < 0.0001$, unpaired t test). These results indicate that deletion of *Shank2* in GABAergic neurons leads to strong repetitive behaviors in multiple tests.

Viaat-Cre;Shank2$^{fl/fl}$ mice show hyperactivity in a novel environment but normal anxiety-like behaviors

We next tested locomotor activity of *Viaat-Cre;Shank2*$^{fl/fl}$ mice in the open-field test, a novel environment. *Viaat-Cre;Shank2*$^{fl/fl}$ mice showed heightened locomotor activity, likely caused by reduced habituation in complete darkness conditions (Fig. 10*A*; interaction, $F_{(5,150)} = 4.34$, $p = 0.0010$; genotype, $F_{(1,30)} = 14.80$, $p = 0.0006$; time, $F_{(5,150)} = 30.11$, $p < 0.0001$, repeated-measures two-way ANOVA for 1 h binned distance moved; $t_{(30)} = 3.846$, $p = 0.0006$, unpaired t test for total distance moved). In the LABORAS test, however, *Viaat-Cre;Shank2*$^{fl/fl}$ mice showed normal locomotion during the first 12 h and the entire 96 h observation period, although a similar hyperactivity was observed during the first 6 h (Fig. 10*B*; interaction, $F_{(94,\ 3478)} = 1.41$, $p = 0.0061$; genotype, $F_{(1,37)} = 0.03$, $p = 0.8716$; time, $F_{(94,\ 3478)} = 28.05$, $p < 0.0001$, repeated-measures two-way ANOVA for 1 h binned distance moved; $t_{(37)} = 2.276$, $p = 0.0287$, unpaired t test for first 6 h; $t_{(37)} = 0.2083$, $p = 0.8361$, unpaired t test for first 12 h; $t_{(37)} = 0.1476$, $p = 0.8834$, unpaired t test for total distance moved). These results suggest that *Viaat-Cre;Shank2*$^{fl/fl}$ mice display hyperactivity in a novel but not in a familiar environment, partly mimicking the strong open-field hyperactivity observed in conventional *Shank2*$^{-/-}$ mice.

In anxiety-like behavioral domains, *Viaat-Cre;Shank2*$^{fl/fl}$ mice showed no detectable abnormalities in an open-field arena ($t_{(30)} = 1.290$, $p = 0.2070$, unpaired t test), elevated plus maze ($t_{(19)} = 0.4472$, $p = 0.6598$ for time in open arms; $t_{(19)} =$

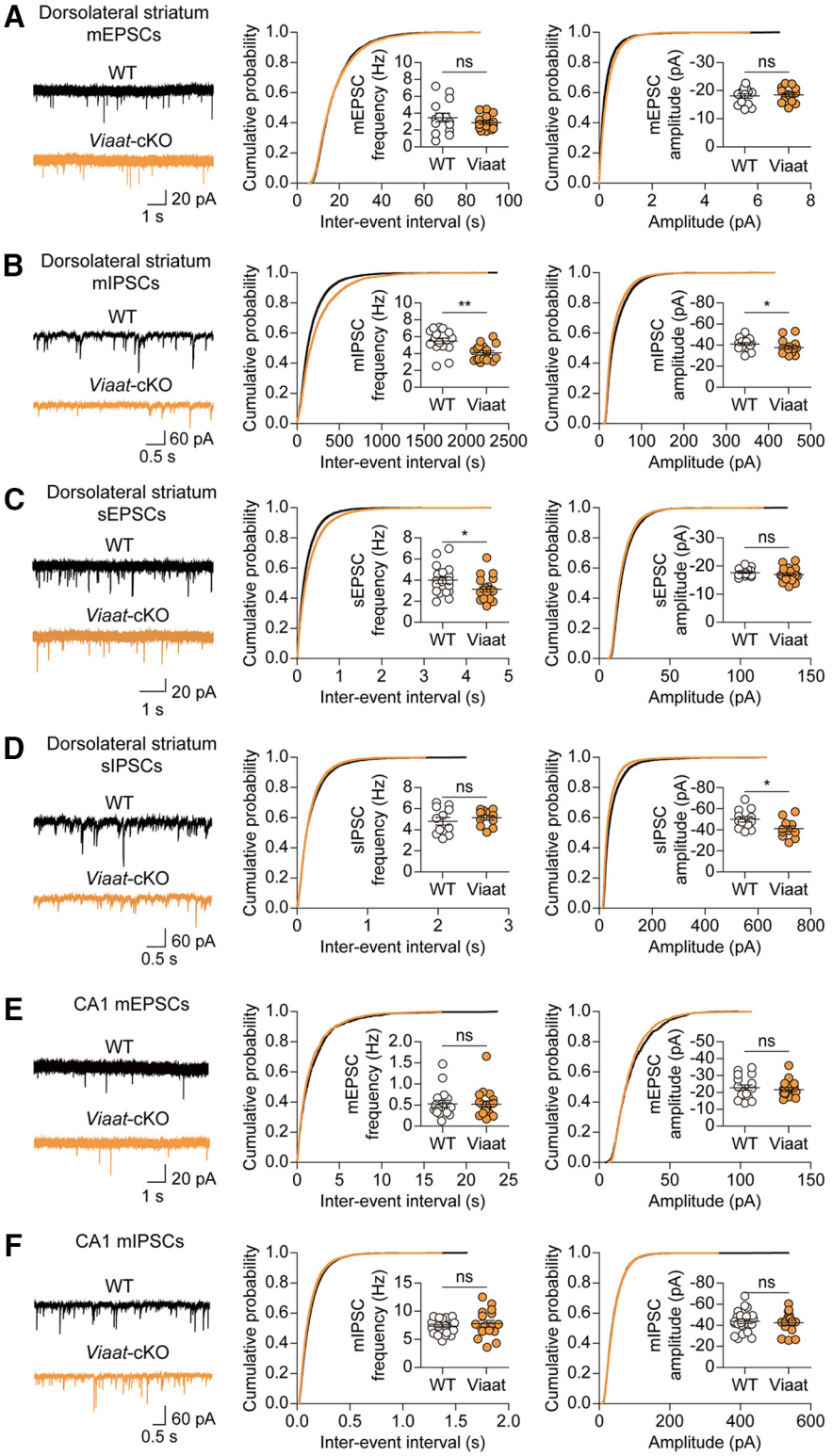

Figure 8. Suppressed inhibitory transmission in the *Viaat-Cre;Shank2*$^{fl/fl}$ striatum. ***A***, ***B***, Normal frequency and amplitude of mEPSCs (***A***) but decreased frequency and amplitude of mIPSCs (***B***) in *Viaat-Cre;Shank2*$^{fl/fl}$ dorsolateral striatal neurons (P30 –P34). $n = 14$ cells from 5 mice for WT and $n = 15$ cells from 4 mice for cKO for mEPSCs and $n = 16$ cells from 4 mice for WT and $n = 17$ cells from 4 mice for cKO for mIPSCs, $^*p < 0.05$, $^{**}p < 0.01$, ns (not significant), Student's t test and Mann–Whitney U test (for mIPSCs). ***C***, ***D***, Decreased frequency but normal amplitude of sEPSCs (***C***) and decreased amplitude but normal frequency of sIPSCs (***D***) in *Viaat-Cre;Shank2*$^{fl/fl}$ dorsolateral striatal neurons (P30 –P34). $n = 18$ cells from 4 mice for WT and $n = 19$ cells from 4 mice for cKO for sEPSCs and $n = 12$ cells from 3 mice for WT and $n = 11$ cells from 3 mice for cKO for sIPSCs, $^*p < 0.05$, ns (not significant), Student's t test. ***E***, ***F***, Normal mEPSCs and mIPSCs in CA1 pyramidal neurons of the *Viaat-Cre;Shank2*$^{fl/fl}$ hippocampus (P21–P25). $n = 17$ cells from 5 mice for WT and $n = 18$ cells from 4 mice for cKO for mEPSC, and $n = 23$ cells from 6 mice for WT and $n = 17$ cells from 6 mice for cKO for mIPSC. ns (not significant), Mann–Whitney U test and Student's t test (for mIPSCs).

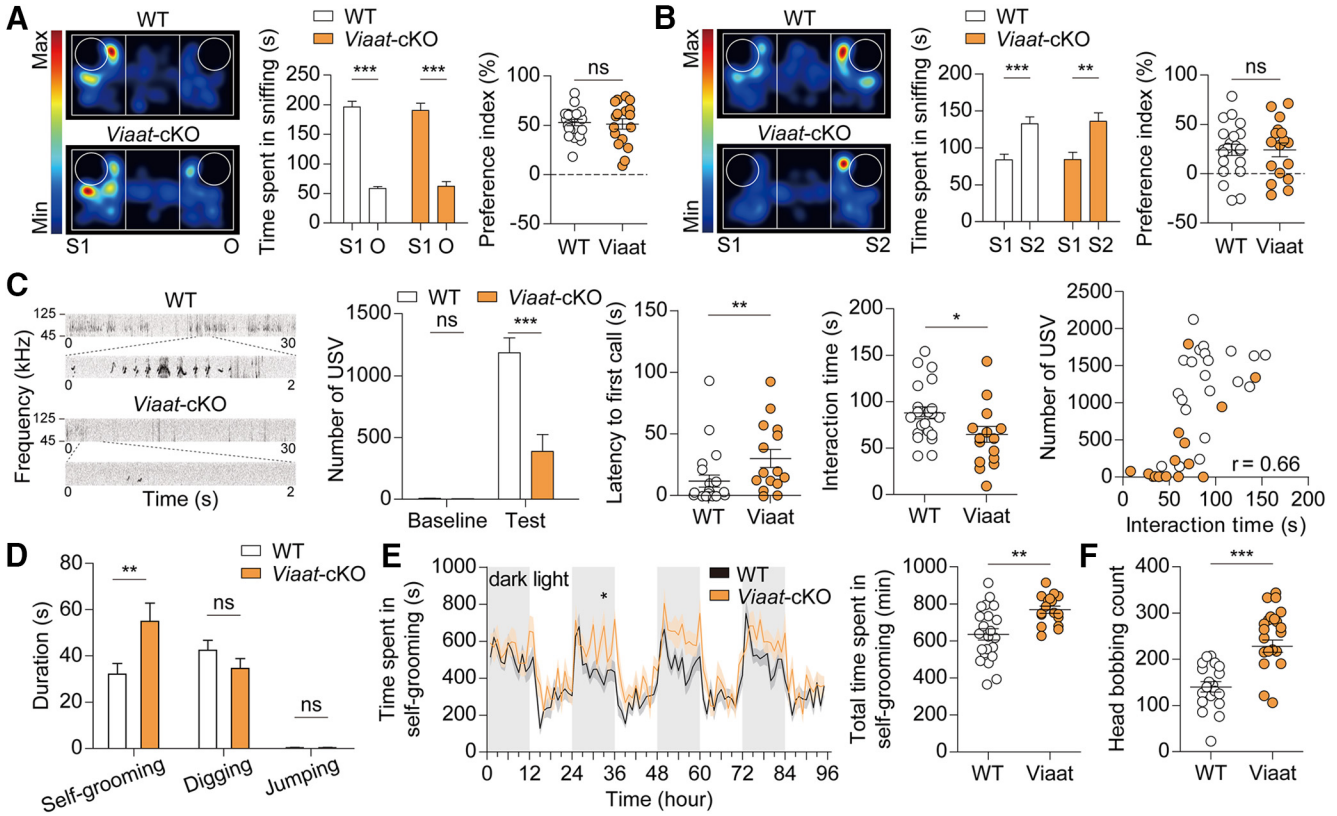

Figure 9. *Viaat-Cre;Shank2*$^{fl/fl}$ mice show normal three-chamber social approach but reduced direct social interaction and USVs and enhanced self-grooming. ***A***, ***B***, Normal social approach (***A***) and social novelty recognition (***B***) in *Viaat-Cre;Shank2*$^{fl/fl}$ mice (9–12 weeks) in the three-chamber test, as shown by time spent in sniffing and the social preference index. $n = 21$ mice for WT and 17 for cKO, $^{**}p < 0.01$, $^{***}p < 0.001$, ns (not significant), Student's *t* test. ***C***, Reduced number of USVs and increased time to emit the first USV in *Viaat-Cre;Shank2*$^{fl/fl}$ mice (10–13 weeks). Note that only female encounter-induced, but not basal, USVs are reduced and that direct male–female social interaction was reduced, as measured by the time spent in sniffing, following, and mounting in males, which shows a positive correlation with the number of USVs ($r = 0.66$; $n = 37$, 22 for WT and 15 for cKO combined, Spearman's correlation). $n = 22$ mice for WT and 15 for cKO, $^{*}p < 0.05$, $^{**}p < 0.01$, $^{***}p < 0.001$, ns (not significant), Mann–Whitney *U* test and Student's *t* test (for interaction time). ***D***, Enhanced self-grooming but normal digging and jumping in *Viaat-Cre;Shank2*$^{fl/fl}$ mice (10–13 weeks) in home cages. $n = 22$ mice for WT and 17 for cKO for self-grooming, digging, and jumping, $^{**}p < 0.01$, ns (not significant), Mann–Whitney *U* test. ***E***, Enhanced self-grooming in *Viaat-Cre;Shank2*$^{fl/fl}$ mice (12–15 weeks) in the LABORAS test. $n = 22$ mice for WT and 17 for cKO, $^{*}p < 0.05$, $^{**}p < 0.01$, two-way ANOVA and Student's *t* test. ***F***, Enhanced head bobbing in *Viaat-Cre;Shank2*$^{fl/fl}$ mice (11–13 weeks) in the hole-board test. $n = 19$ mice for WT and 21 for cKO, $^{***}p < 0.001$, Student's *t* test.

0.6248, $p = 0.5396$ for time in closed arms, unpaired *t* test for all), or light–dark apparatus ($t_{(22)} = 1.387$, $p = 0.1793$ for time in light chamber; $t_{(22)} = 0.8289$, $p = 0.4160$ for number of transitions, unpaired *t* test for all; Fig. 10*A*,*C*,*D*). These results indicate that the anxiety-like behaviors observed in conventional *Shank2*$^{-/-}$ mice are also observed in *CaMKII-Cre;Shank2*$^{fl/fl}$ mice, albeit with some specific differences, but not in *Viaat-Cre;Shank2*$^{fl/fl}$ mice.

To determine whether the *Viaat-Cre* background has any influences on the behavioral phenotypes of *Viaat-Cre;Shank2*$^{fl/fl}$ mice, we subjected *Viaat-Cre* mice to several behavioral tests in which *Viaat-Cre;Shank2*$^{fl/fl}$ mice showed behavioral alterations. *Viaat-Cre* mice showed normal levels of USVs ($U = 31.00$, $p = 0.9534$, for number of calls during baseline periods; $U = 16.00$, $p = 0.1049$, for number of calls during test periods, Mann–Whitney *U* test for both; $t_{(14)} = 1.260$, $p = 0.2283$, unpaired *t* test for latency to the first call), social interaction during USVs ($t_{(14)} = 1.240$, $p = 0.2353$, unpaired *t* test for interaction time; $r = 0.7438$, $p = 0.0010$, Pearson's correlation for correlational analysis of interaction time and number of calls), self-grooming (home cage, $U = 29.00$, $p = 0.5414$, Mann–Whitney *U* test) and LABORAS (interaction, $F_{(94,1504)} = 0.89$, $p = 0.7691$; genotype, $F_{(1,16)} = 0.22$, $p = 0.6424$; time, $F_{(94,1504)} = 5.65$, $p < 0.0001$, repeated-measures two-way ANOVA for 1 h binned grooming duration; $t_{(16)} = 0.4733$ $p = 0.6424$, unpaired *t* test for total grooming duration), hole-board head bobbing ($U = 25.50$, $p = 0.2126$, Mann–Whitney *U* test), and locomotor activity (open-field (interaction, $F_{(5,95)} = 2.30$, $p = 0.0513$; genotype, $F_{(1,19)} = 0.51$, $p = 0.4841$; time, $F_{(5,95)} = 74.54$, $p < 0.0001$, repeated-measures two-way ANOVA for 1 h binned distance moved; $t_{(19)} = 0.7136$, $p = 0.4841$, unpaired *t* test for total distance moved; $t_{(19)} = 1.985$, $p = 0.0618$, unpaired *t* test for time in center), and LABORAS (interaction, $F_{(94,1504)} = 1.10$, $p = 0.2394$; genotype, $F_{(1,16)} = 0.00$, $p = 0.9998$; time, $F_{(94,1504)} = 14.97$, $p < 0.0001$, repeated-measures two-way ANOVA for 1 h binned distance moved; $U = 32.00$, $p = 0.5148$, Mann–Whitney *U* test for first 6 h; $U = 34.00$, $p = 0.6334$, Mann–Whitney *U* test for first 12 h; $t_{(16)} = 0.0003$, $p = 0.9998$, unpaired *t* test for total distance moved); Fig. 11*A*–*F*).

Discussion

In the present study, we investigated the effects of cell-type-specific *Shank2* deletion restricted to excitatory and inhibitory neurons on synaptic and behavioral phenotypes in mice. We found that these cell-type-specific *Shank2* deletions cause distinct alterations in synaptic transmission and behaviors in social, repetitive, locomotor, and anxiety-like domains (behavioral phenotypes are summarized in Table 1).

Specifically, three-chamber social-approach deficits observed in conventional *Shank2*$^{-/-}$ mice were also observed in *CaMKII-*

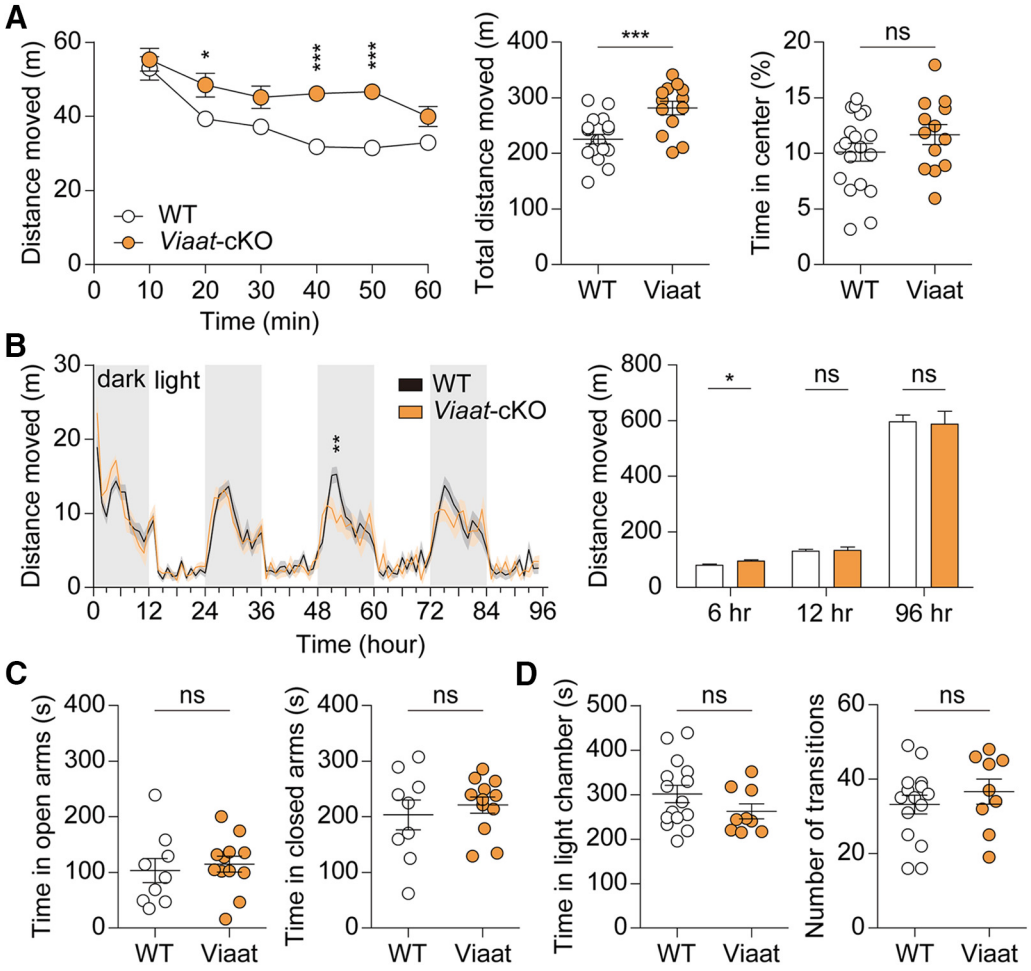

Figure 10. *Viaat-Cre;Shank2*$^{fl/fl}$ mice show hyperactivity in a novel environment but normal anxiety-like behaviors. ***A***, Hyperactivity of *Viaat-Cre;Shank2*$^{fl/fl}$ mice (9–12 weeks) in the open-field test (a novel environment) under a complete darkness (0 lux) condition. Note that *Viaat-Cre;Shank2*$^{fl/fl}$ mice spend a normal amount of time in the center region. $n = 19$ for WT and 13 for cKO, $^{*}p < 0.05$, $^{***}p < 0.001$, ns (not significant), two-way ANOVA and Student's *t* test. ***B***, Normal locomotor activity of *Viaat-Cre;Shank2*$^{fl/fl}$ mice (12–15 weeks) in the LABORAS test (a familiar environment) during the first 12 and 96 h. Note, however, that locomotor activity during the first 6 h, a time period when the environment is likely more novel compared with later hours, is enhanced. $n = 22$ mice for WT and 17 for cKO, $^{*}p < 0.05$, $^{**}p < 0.01$, ns (not significant), two-way ANOVA and Student's *t* test. ***C***, Normal anxiety-like behavior of *Viaat-Cre;Shank2*$^{fl/fl}$ mice (11–14 weeks) in the elevated plus maze test. $n = 9$ mice for WT and 12 for cKO, ns (not significant), Student's *t* test. ***D***, Normal anxiety-like behavior of *Viaat-Cre;Shank2*$^{fl/fl}$ mice (11–14 weeks) in the light– dark test. $n = 15$ mice for WT and 9 for cKO, ns (not significant), Student's *t* test.

Cre;Shank2$^{fl/fl}$ mice, but not in *Viaat-Cre;Shank2*$^{fl/fl}$ mice. In contrast, the social communication deficits (abnormal USVs) characteristic of *Shank2*$^{-/-}$ mice were observed in *Viaat-Cre;Shank2*$^{fl/fl}$ mice, whereas *CaMKII-Cre;Shank2*$^{fl/fl}$ mice showed much weaker deficits. These results suggest that *Shank2* deletion in excitatory and inhibitory neurons leads to stronger deficits in three-chamber social approach and USVs, respectively. Direct male–female social interaction during the USV test was reduced in both *CaMKII-Cre;Shank2*$^{fl/fl}$ and *Viaat-Cre;Shank2*$^{fl/fl}$ mice. This contrasts with the social approach deficits strongly observed in *CaMKII-Cre;Shank2*$^{fl/fl}$, but not in *Viaat-Cre;Shank2*$^{fl/fl}$ mice. This difference could be attributable to the distinct contexts of the tests used such as social approach versus direct social interaction or male–male versus male–female interaction.

Viaat-Cre;Shank2$^{fl/fl}$ mice showed strong repetitive behaviors, displaying enhanced self-grooming in both their home and LABORAS cages and also displaying enhanced head bobbing in the hole-board test. In contrast, these repetitive behaviors were not observed in conventional *Shank2*$^{-/-}$ mice or *CaMKII-Cre;Shank2*$^{fl/fl}$ mice. It is possible that the enhanced self-grooming and head-bobbing behaviors caused by GABAergic *Shank2* deletion are suppressed by global gene deletion in conventional *Shank2*$^{-/-}$ mice. Reduced digging was observed in both *CaMKII-Cre;Shank2*$^{fl/fl}$ mice, but not in *Viaat-Cre;Shank2*$^{fl/fl}$ mice, similar to conventional *Shank2*$^{-/-}$ mice, suggesting that *Shank2* deletion in excitatory neurons may control digging control. Regarding potential circuit mechanisms underlying the enhanced repetitive behaviors in *Viaat-Cre;Shank2*$^{fl/fl}$ mice, they could be changes occurring in the striatum, a brain region strongly associated with motor control and motivational behaviors. However, repetitive behaviors in mice have also been shown to involve many other brain regions such as cortex, hypothalamus, amygdala, cerebellum, and brainstem (Kruk et al., 1998; Burguière et al., 2013; Hong et al., 2014; Kalueff et al., 2016).

Contributions of excitatory and/or inhibitory neurons to two core autistic-like behaviors, social deficits and repetitive behavior, have been tested previously in several mouse models of ASD. For instance, social interaction deficits in the three-chamber test have been observed in mice carrying CaMKII-specific deletion of ASD-risk genes including *Apc* (Mohn et al., 2014), *Atg7* (Tang et al., 2014), *Cc2d1a* (Oaks et al., 2017), and *Mecp2* (Gemelli et al., 2006). It is interesting that deletion of these genes restricted to

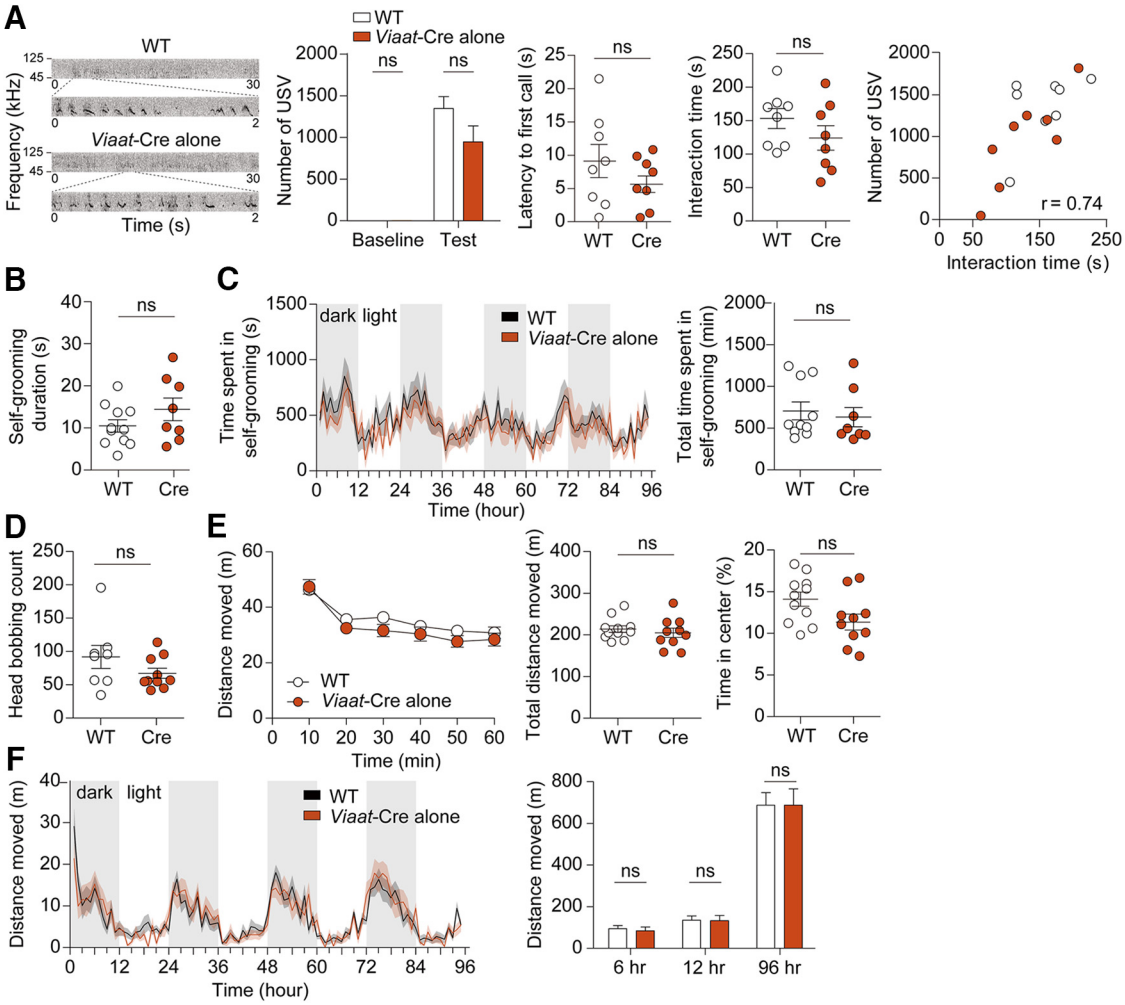

Figure 11. *Viaat-Cre* mice show normal USVs, self-grooming, hole-board head bobbing, and locomotor activity. ***A***, Normal numbers of USVs (basal and female encounter) and latency to first call in *Viaat-Cre* mice (11 weeks; males). Note that direct male–female social interaction is normal in *Viaat-Cre* mice, as measured by the time spent in sniffing, following, and mounting in males, which shows a positive correlation with the number of USVs ($r = 0.74$, $n = 16$, WT and Viaat-Cre combined, Pearson's correlation). $n = 8$ mice for WT and Viaat-Cre, ns (not significant), Mann–Whitney *U* test (for number of USVs) and Student's *t* test. ***B***, Normal self-grooming in *Viaat-Cre* mice (11 weeks) in home cages. $n = 9$ mice for WT and 8 for Viaat-Cre, ns (not significant), Mann–Whitney *U* test. ***C***, Normal self-grooming in *Viaat-Cre* mice (11 weeks) in the LABORAS test. $n = 10$ mice for WT and 8 for Viaat-Cre, ns (not significant), two-way ANOVA and Student's *t* test. ***D***, Normal head bobbing in *Viaat-Cre* mice (11–13 weeks) in the hole-board test. $n = 8$ mice for WT and 10 for Viaat-Cre, ns (not significant), Student's *t* test. ***E***, Normal locomotor activity of *Viaat-Cre* mice (11–12 weeks) in the open-field test under complete darkness (0 lux) condition. Note that these mice also show normal anxiety-like behavior, as shown by the normal time spent in the center region of the open-field arena. $n = 11$ for WT and 10 for Viaat-Cre, ns (not significant), two-way ANOVA and Student's *t* test. ***F***, Normal self-grooming in *Viaat-Cre* mice (11 weeks) in the LABORAS test. $n = 10$ mice for WT and 8 for cKO, ns (not significant), two-way ANOVA and Student's *t* test.

Table 1. Summary of behavioral phenotypes of conventional *Shank2*$^{-/-}$ and *Shank2* conditional mice

Behavioral domain	Behavioral test	*Shank2* KO	*CaMKII*-cKO	*Viaat*-cKO
Social behavior	Three-chamber social approach (male–male)	↓ ↓	↓ ↓	—
	Adult USV	↓ ↓ ↓	↓	↓ ↓ ↓
	Direct interaction (male–female)		↓ ↓	↓ ↓
Repetitive behavior	Self-grooming	—	—	↑ ↑
	LABORAS self-grooming	—	—	↑ ↑
	Digging	↓ ↓ ↓	↓ ↓ ↓	—
	Jumping	↑ ↑	—	—
	Hole-board test	—	—	↑ ↑ ↑
Locomotor activity	Open-field test	↑ ↑ ↑	↑ ↑	↑ ↑
	LABORAS test	↑ ↑	↑	↑
Anxiety-like behavior	Open-field test (center)	—	↑ ↑	—
	Elevated plus maze	↑ ↑	—	—
	Light– dark test	—	↑ ↑	—

This table summarizes only the increases or decreases of various behaviors in a given conditional mouse line relative to WT mice and is not intended for comparison of the extent of changes in a single behavior across different mouse lines. Empty field, Not measured; -, no change; up and down arrows, increases and decreases, respectively; one, two, and three arrows, moderate, mid-level, and strong changes, respectively. Data for conventional *Shank2*$^{-/-}$ mice have been published previously (Won et al., 2012).

CaMKII-positive excitatory neurons, despite their diverse protein functions, seems to frequently cause social interaction deficits similar to *CaMKII-Cre;Shank2*$^{fl/fl}$ mice. However, tests of these mouse models for repetitive behaviors yielded variable results: enhanced digging in *Apc*-mutant mice (Mohn et al., 2014), enhanced self-grooming in *Cc2d1a*-mutant mice (Oaks et al., 2017), but normal self-grooming in *Atg7*-mutant mice (Tang et al., 2014).

Several ASD risk genes have also been deleted in GABAergic neurons using Cre recombination driven by Gad2, Viaat, Dlx1/2, or Dlx5/6 promoters. Some of these mouse lines exhibit altered repetitive behaviors and social interaction/communication deficits. Specific examples of alterations in repetitive behaviors include increased hole-board head bobbing in *Viaat-Mecp2* and *Dlx5/6-Mecp2* mice (Chao et al., 2010) and increased repetitive circling in *Dlx1/2-Scn1a* mice (Han et al., 2012). These results are similar to the increased self-grooming and hole-board head bobbing in our *Viaat-Cre;Shank2*$^{fl/fl}$ mice. In contrast, the same gene deletions cause variable degrees of social deficits: increased social interaction in *Viaat-Mecp2* and *Dlx5/6-Mecp2* mice (three-chamber and partition test; Chao et al., 2010), but decreased social interaction in *Dlx1/2-Scn1a* mice (three-chamber; Han et al., 2012). Therefore, it is tempting to speculate that deletion of ASD risk genes in excitatory neurons is frequently associated with social interaction deficits, whereas deletion of these genes in inhibitory neurons is associated with repetitive behaviors, although care should be taken and further studies are required given the substantial diversity of excitatory and inhibitory neurons in the brain.

Strong hyperactivity is a phenotype characteristic of conventional *Shank2*$^{-/-}$ mice (Schmeisser et al., 2012; Won et al., 2012). However, *CaMKII-Cre;Shank2*$^{fl/fl}$ mice showed mild hyperactivity in both the open-field arena and LABORAS cages. *Viaat-Cre;Shank2*$^{fl/fl}$ mice also showed mild hyperactivity in the open-field arena, but normal locomotor activity in LABORAS cages. It is possible that *Shank2* deletion in both excitatory and inhibitory neurons additively contributes to the strong hyperactivity observed in conventional *Shank2*$^{-/-}$ mice or cell types other than just excitatory and inhibitory such as modulatory might be important.

In the anxiety-related behavioral domain, *CaMKII-Cre;Shank2*$^{fl/fl}$ mice show enhanced anxiety-like behaviors in an open-field arena and a light–dark apparatus, but not in an elevated plus maze. An almost complementary pattern is observed in conventional *Shank2*$^{-/-}$ mice, which show anxiety-like behavior in the elevated plus maze, but not in an open-field area or a light–dark apparatus (Won et al., 2012). It appears that *Shank2* deletion in excitatory neurons leads to distinct anxiety-like behaviors that are not observed in conventional *Shank2*$^{-/-}$ mice. In contrast, *Shank2* deletion in GABAergic neurons in *Viaat-Cre;Shank2*$^{fl/fl}$ mice minimally affected anxiety-like behaviors, although the diversity of GABAergic cell types should be considered.

In addition to behavioral modulation, our results point to a role for Shank2 in regulating excitatory and inhibitory synaptic transmission in distinct brain regions. Specifically, *CaMKII-Cre;Shank2*$^{fl/fl}$ mice show reduced frequency of mEPSCs in hippocampal CA1 pyramidal neurons. Given that paired-pulse facilitation is normal at these *CaMKII-Cre;Shank2*$^{fl/fl}$ SC-CA1 synapses, postsynaptic removal of *Shank2* is likely to cause a reduction in the number of excitatory synapses. In addition, it should be pointed out that conventional *Shank2*$^{-/-}$ mice do not show altered mEPSCs in the same CA1 pyramidal neurons (Won et al., 2012). These results suggest that the reduced mEPSC frequency in *CaMKII-Cre;Shank2*$^{fl/fl}$ mice caused by excitatory neuron-restricted *Shank2* deletion might be suppressed by global *Shank2* KO.

Our results also indicate that *Viaat-Cre;Shank2*$^{fl/fl}$ mice display significant decreases in the frequency and amplitude of mIPSCs in dorsolateral striatal neurons, effects not observed in hippocampal neurons. The decreased mIPSC frequency may be attributable to suppressed inhibitory synaptic input from neighboring *Shank2*-deficient GABAergic striatal neurons because it is known that the majority of inhibitory input onto MSNs, the most abundant cell type in the striatum, comes from neighboring MSNs (Guzmán et al., 2003). A result that is not easy to interpret is the decrease in mIPSC amplitude, which is normally attributable to postsynaptic changes. It is possible that the presynaptic changes induced by *Shank2* deletion might have *trans*-synaptically caused a decrease in mIPSC amplitude. Alternatively, it could stem indirectly from excitatory synaptic changes in the same postsynaptic neuron, as supported by the decreased sEPSC frequency in these neurons. The latter could be caused by suppressed activity of upstream excitatory neurons involving altered network activity, although further details remain to be determined.

In conclusion, our data suggest that *Shank2* deletion restricted to excitatory and inhibitory neurons leads to distinct synaptic and behavioral phenotypes in mice, pointing to cell-type-specific Shank2-dependent regulation of neuronal synapses and behaviors.

References

Berkel S, Tang W, Treviño M, Vogt M, Obenhaus HA, Gass P, Scherer SW, Sprengel R, Schratt G, Rappold GA (2012) Inherited and de novo SHANK2 variants associated with autism spectrum disorder impair neuronal morphogenesis and physiology. Hum Mol Genet 21:344–357. CrossRef Medline

Bockmann J, Kreutz MR, Gundelfinger ED, Böckers TM (2002) ProSAP/Shank postsynaptic density proteins interact with insulin receptor tyrosine kinase substrate IRSp53. J Neurochem 83:1013–1017. CrossRef Medline

Boeckers TM, Bockmann J, Kreutz MR, Gundelfinger ED (2002) ProSAP/Shank proteins: a family of higher order organizing molecules of the postsynaptic density with an emerging role in human neurological disease. J Neurochem 81:903–910. CrossRef Medline

Boeckers TM, Winter C, Smalla KH, Kreutz MR, Bockmann J, Seidenbecher C, Garner CC, Gundelfinger ED (1999a) Proline-rich synapse-associated proteins ProSAP1 and ProSAP2 interact with synaptic proteins of the SAPAP/GKAP family. Biochem Biophys Res Commun 264:247–252. CrossRef Medline

Boeckers TM, Kreutz MR, Winter C, Zuschratter W, Smalla KH, Sanmarti-Vila L, Wex H, Langnaese K, Bockmann J, Garner CC, Gundelfinger ED (1999b) Proline-rich synapse-associated protein-1/cortactin binding protein 1 (ProSAP1/CortBP1) is a PDZ-domain protein highly enriched in the postsynaptic density. J Neurosci 19:6506–6518. Medline

Burguière E, Monteiro P, Feng G, Graybiel AM (2013) Optogenetic stimulation of lateral orbitofronto-striatal pathway suppresses compulsive behaviors. Science 340:1243–1246. CrossRef Medline

Cepeda C, André VM, Yamazaki I, Wu N, Kleiman-Weiner M, Levine MS (2008) Differential electrophysiological properties of dopamine D1 and D2 receptor-containing striatal medium-sized spiny neurons. Eur J Neurosci 27:671–682. CrossRef Medline

Cepeda C, Colwell CS, Itri JN, Chandler SH, Levine MS (1998) Dopaminergic modulation of NMDA-induced whole cell currents in neostriatal neurons in slices: contribution of calcium conductances. J Neurophysiol 79:82–94. CrossRef Medline

Chao HT, Chen H, Samaco RC, Xue M, Chahrour M, Yoo J, Neul JL, Gong S, Lu HC, Heintz N, Ekker M, Rubenstein JL, Noebels JL, Rosenmund C, Zoghbi HY (2010) Dysfunction in GABA signalling mediates autism-like stereotypies and rett syndrome phenotypes. Nature 468:263–269. CrossRef Medline

Chilian B, Abdollahpour H, Bierhals T, Haltrich I, Fekete G, Nagel I, Rosenberger G, Kutsche K (2013) Dysfunction of SHANK2 and CHRNA7 in a patient with intellectual disability and language impairment supports genetic epistasis of the two loci. Clin Genet 84:560–565. CrossRef Medline

Costas J (2015) The role of SHANK2 rare variants in schizophrenia susceptibility. Mol Psychiatry 20:1486. CrossRef Medline

Dere E, Winkler D, Ritter C, Ronnenberg A, Poggi G, Patzig J, Gernert M, Müller C, Nave KA, Ehrenreich H, Werner HB (2015) Gpm6b deficiency impairs sensorimotor gating and modulates the behavioral response to a 5-HT2A/C receptor agonist. Behav Brain Res 277:254–263. CrossRef Medline

Du Y, Weed SA, Xiong WC, Marshall TD, Parsons JT (1998) Identification of a novel cortactin SH3 domain-binding protein and its localization to growth cones of cultured neurons. Mol Cell Biol 18:5838–5851. CrossRef Medline

Egnor SR, Seagraves KM (2016) The contribution of ultrasonic vocalizations to mouse courtship. Curr Opin Neurobiol 38:1–5. CrossRef Medline

Ey E, Torquet N, Le Sourd AM, Leblond CS, Boeckers TM, Faure P, Bourgeron T (2013) The autism ProSAP1/Shank2 mouse model displays quantitative and structural abnormalities in ultrasonic vocalisations. Behav Brain Res 256:677–689. CrossRef Medline

Gemelli T, Berton O, Nelson ED, Perrotti LI, Jaenisch R, Monteggia LM (2006) Postnatal loss of methyl-CpG binding protein 2 in the forebrain is sufficient to mediate behavioral aspects of rett syndrome in mice. Biol Psychiatry 59:468–476. CrossRef Medline

Gertler TS, Chan CS, Surmeier DJ (2008) Dichotomous anatomical properties of adult striatal medium spiny neurons. J Neurosci 28:10814–10824. CrossRef Medline

Grabrucker AM (2014) A role for synaptic zinc in ProSAP/Shank PSD scaffold malformation in autism spectrum disorders. Dev Neurobiol 74:136–146. CrossRef Medline

Grabrucker AM, Schmeisser MJ, Schoen M, Boeckers TM (2011) Postsynaptic ProSAP/Shank scaffolds in the cross-hair of synaptopathies. Trends Cell Biol 21:594–603. CrossRef Medline

Guilmatre A, Huguet G, Delorme R, Bourgeron T (2014) The emerging role of SHANK genes in neuropsychiatric disorders. Dev Neurobiol 74:113–122. CrossRef Medline

Guzmán JN, Hernández A, Galarraga E, Tapia D, Laville A, Vergara R, Aceves J, Bargas J (2003) Dopaminergic modulation of axon collaterals interconnecting spiny neurons of the rat striatum. J Neurosci 23:8931–8940. Medline

Ha S, Lee D, Cho YS, Chung C, Yoo YE, Kim J, Lee J, Kim W, Kim H, Bae YC, Tanaka-Yamamoto K, Kim E (2016) Cerebellar Shank2 regulates excitatory synapse density, motor coordination, and specific repetitive and anxiety-like behaviors. J Neurosci 36:12129–12143. CrossRef Medline

Han S, Yu FH, Schwartz MD, Linton JD, Bosma MM, Hurley JB, Catterall WA, de la Iglesia HO (2012) Na(V)1.1 channels are critical for intercellular communication in the suprachiasmatic nucleus and for normal circadian rhythms. Proc Natl Acad Sci U S A 109:E368–E377. CrossRef Medline

Harony-Nicolas H, De Rubeis S, Kolevzon A, Buxbaum JD (2015) Phelan McDermid syndrome: from genetic discoveries to animal models and treatment. J Child Neurol 30:1861–1870. CrossRef Medline

Hayashi MK, Tang C, Verpelli C, Narayanan R, Stearns MH, Xu RM, Li H, Sala C, Hayashi Y (2009) The postsynaptic density proteins homer and shank form a polymeric network structure. Cell 137:159–171. CrossRef Medline

Heise C, Schroeder JC, Schoen M, Halbedl S, Reim D, Woelfle S, Kreutz MR, Schmeisser MJ, Boeckers TM (2016) Selective localization of shanks to VGLUT1-positive excitatory synapses in the mouse hippocampus. Front Cell Neurosci 10:106. CrossRef Medline

Homann OR, Misura K, Lamas E, Sandrock RW, Nelson P, McDonough SI, DeLisi LE (2016) Whole-genome sequencing in multiplex families with psychoses reveals mutations in the SHANK2 and SMARCA1 genes segregating with illness. Mol Psychiatry 21:1690–1695. CrossRef Medline

Hong W, Kim DW, Anderson DJ (2014) Antagonistic control of social versus repetitive self-grooming behaviors by separable amygdala neuronal subsets. Cell 158:1348–1361. CrossRef Medline

Hulbert SW, Jiang YH (2016) Monogenic mouse models of autism spectrum disorders: common mechanisms and missing links. Neuroscience 321:3–23. Medline

Jiang YH, Ehlers MD (2013) Modeling autism by SHANK gene mutations in mice. Neuron 78:8–27. CrossRef Medline

Kalueff AV, Stewart AM, Song C, Berridge KC, Graybiel AM, Fentress JC (2016) Neurobiology of rodent self-grooming and its value for translational neuroscience. Nat Rev Neurosci 17:45–59. CrossRef Medline

Kruk MR, Westphal KG, Van Erp AM, van Asperen J, Cave BJ, Slater E, de Koning J, Haller J (1998) The hypothalamus: cross-roads of endocrine and behavioural regulation in grooming and aggression. Neurosci Biobehav Rev 23:163–177. CrossRef Medline

Leblond CS, Heinrich J, Delorme R, Proepper C, Betancur C, Huguet G, Konyukh M, Chaste P, Ey E, Rastam M, Anckarsäter H, Nygren G, Gillberg IC, Melke J, Toro R, Regnault B, Fauchereau F, Mercati O, Lemière N, Skuse D, et al. (2012) Genetic and functional analyses of SHANK2 mutations suggest a multiple hit model of autism spectrum disorders. PLoS Genet 8:e1002521. CrossRef Medline

Leblond CS, Nava C, Polge A, Gauthier J, Huguet G, Lumbroso S, Giuliano F, Stordeur C, Depienne C, Mouzat K, Pinto D, Howe J, Lemière N, Durand CM, Guibert J, Ey E, Toro R, Peyre H, Mathieu A, Amsellem F, et al. (2014) Meta-analysis of SHANK Mutations in Autism Spectrum Disorders: a gradient of severity in cognitive impairments. PLoS Genet 10:e1004580. CrossRef Medline

Lee EJ, Choi SY, Kim E (2015a) NMDA receptor dysfunction in autism spectrum disorders. Curr Opin Pharmacol 20:8–13. CrossRef Medline

Lee EJ, Lee H, Huang TN, Chung C, Shin W, Kim K, Koh JY, Hsueh YP, Kim E (2015b) Trans-synaptic zinc mobilization improves social interaction in two mouse models of autism through NMDAR activation. Nat Commun 6:7168. CrossRef Medline

Lee J, Chung C, Ha S, Lee D, Kim DY, Kim H, Kim E (2015c) Shank3-mutant mice lacking exon 9 show altered excitation/inhibition balance, enhanced rearing, and spatial memory deficit. Front Cell Neurosci 9:94. CrossRef Medline

Lim CS, Kim H, Yu NK, Kang SJ, Kim T, Ko HG, Lee J, Yang JE, Ryu HH, Park T, Gim J, Nam HJ, Baek SH, Wegener S, Schmitz D, Boeckers TM, Lee MG, Kim E, Lee JH, et al. (2017) Enhancing inhibitory synaptic function reverses spatial memory deficits in Shank2 mutant mice. Neuropharmacology 112:104–112. CrossRef Medline

Lim S, Naisbitt S, Yoon J, Hwang JI, Suh PG, Sheng M, Kim E (1999) Characterization of the shank family of synaptic proteins. multiple genes, alternative splicing, and differential expression in brain and development. J Biol Chem 274:29510–29518. CrossRef Medline

MacGillavry HD, Kerr JM, Kassner J, Frost NA, Blanpied TA (2016) Shank-cortactin interactions control actin dynamics to maintain flexibility of neuronal spines and synapses. Eur J Neurosci 43:179–193. CrossRef Medline

Maggio JC, Whitney G (1985) Ultrasonic vocalizing by adult female mice (*Mus musculus*). J Comp Psychol 99:420–436. CrossRef Medline

Mohn JL, Alexander J, Pirone A, Palka CD, Lee SY, Mebane L, Haydon PG, Jacob MH (2014) Adenomatous polyposis coli protein deletion leads to cognitive and autism-like disabilities. Mol Psychiatry 19:1133–1142. CrossRef Medline

Monteiro P, Feng G (2017) SHANK proteins: roles at the synapse and in autism spectrum disorder. Nat Rev Neurosci 18:147–157. CrossRef Medline

Naisbitt S, Kim E, Tu JC, Xiao B, Sala C, Valtschanoff J, Weinberg RJ, Worley PF, Sheng M (1999) Shank, a novel family of postsynaptic density proteins that binds to the NMDA receptor/PSD-95/GKAP complex and cortactin. Neuron 23:569–582. CrossRef Medline

Oaks AW, Zamarbide M, Tambunan DE, Santini E, Di Costanzo S, Pond HL, Johnson MW, Lin J, Gonzalez DM, Boehler JF, Wu GK, Klann E, Walsh CA, Manzini MC (2017) Cc2d1a loss of function disrupts functional and morphological development in forebrain neurons leading to cognitive and social deficits. Cereb Cortex 27:1670–1685. CrossRef Medline

Pappas AL, Bey AL, Wang X, Rossi M, Kim YH, Yan H, Porkka F, Duffney LJ, Phillips SM, Cao X, Ding JD, Rodriguiz RM, Yin HH, Weinberg RJ, Ji RR, Wetsel WC, Jiang YH (2017) Deficiency of Shank2 causes mania-like behavior that responds to mood stabilizers. JCI Insight 2: pii: 92052. CrossRef Medline

Park E, Na M, Choi J, Kim S, Lee JR, Yoon J, Park D, Sheng M, Kim E (2003) The shank family of postsynaptic density proteins interacts with and promotes synaptic accumulation of the beta PIX guanine nucleotide exchange factor for Rac1 and Cdc42. J Biol Chem 278:19220–19229. CrossRef Medline

Peter S, Ten Brinke MM, Stedehouder J, Reinelt CM, Wu B, Zhou H, Zhou K, Boele HJ, Kushner SA, Lee MG, Schmeisser MJ, Boeckers TM, Schonewille M, Hoebeek FE, De Zeeuw CI (2016) Dysfunctional cerebellar purkinje cells contribute to autism-like behaviour in Shank2-deficient mice. Nat Commun 7:12627. CrossRef Medline

Peykov S, Berkel S, Degenhardt F, Rietschel M, Nöthen MM, Rappold GA (2015a) Rare SHANK2 variants in schizophrenia. Mol Psychiatry 20: 1487–1488. CrossRef Medline

Peykov S, Berkel S, Schoen M, Weiss K, Degenhardt F, Strohmaier J, Weiss B, Proepper C, Schratt G, Nöthen MM, Boeckers TM, Rietschel M, Rappold GA (2015b) Identification and functional characterization of rare SHANK2 variants in schizophrenia. Mol Psychiatry 20:1489–1498. CrossRef Medline

Pinto D, Pagnamenta AT, Klei L, Anney R, Merico D, Regan R, Conroy J, Magalhaes TR, Correia C, Abrahams BS, Almeida J, Bacchelli E, Bader GD, Bailey AJ, Baird G, Battaglia A, Berney T, Bolshakova N, Bölte S, Bolton PF, et al. (2010) Functional impact of global rare copy number variation in autism spectrum disorders. Nature 466:368–372. CrossRef Medline

Prasad A, Merico D, Thiruvahindrapuram B, Wei J, Lionel AC, Sato D, Rickaby J, Lu C, Szatmari P, Roberts W, Fernandez BA, Marshall CR, Hatchwell E, Eis PS, Scherer SW (2012) A discovery resource of rare copy number variations in individuals with autism spectrum disorder. G3 (Bethesda) 2:1665–1685. CrossRef Medline

Proepper C, Johannsen S, Liebau S, Dahl J, Vaida B, Bockmann J, Kreutz MR, Gundelfinger ED, Boeckers TM (2007) Abelson interacting protein 1 (Abi-1) is essential for dendrite morphogenesis and synapse formation. EMBO J 26:1397–1409. CrossRef Medline

Qualmann B, Boeckers TM, Jeromin M, Gundelfinger ED, Kessels MM (2004) Linkage of the actin cytoskeleton to the postsynaptic density via direct interactions of Abp1 with the ProSAP/Shank family. J Neurosci 24:2481–2495. CrossRef Medline

Quinn LP, Stean TO, Trail B, Duxon MS, Stratton SC, Billinton A, Upton N (2003) LABORAS: initial pharmacological validation of a system allowing continuous monitoring of laboratory rodent behaviour. J Neurosci Methods 130:83–92. CrossRef Medline

Quinn LP, Stean TO, Chapman H, Brown M, Vidgeon-Hart M, Upton N, Billinton A, Virley DJ (2006) Further validation of LABORAS using various dopaminergic manipulations in mice including MPTP-induced nigro-striatal degeneration. J Neurosci Methods 156:218–227. CrossRef Medline

Rauch A, Wieczorek D, Graf E, Wieland T, Endele S, Schwarzmayr T, Albrecht B, Bartholdi D, Beygo J, Di Donato N, Dufke A, Cremer K, Hempel M, Horn D, Hoyer J, Joset P, Röpke A, Moog U, Riess A, Thiel CT, et al. (2012) Range of genetic mutations associated with severe non-syndromic sporadic intellectual disability: an exome sequencing study. Lancet 380:1674–1682. CrossRef Medline

Romorini S, Piccoli G, Jiang M, Grossano P, Tonna N, Passafaro M, Zhang M, Sala C (2004) A functional role of postsynaptic density-95-guanylate kinase-associated protein complex in regulating shank assembly and stability to synapses. J Neurosci 24:9391–9404. CrossRef Medline

Sala C, Vicidomini C, Bigi I, Mossa A, Verpelli C (2015) Shank synaptic scaffold proteins: keys to understanding the pathogenesis of autism and other synaptic disorders. J Neurochem 135:849–858. CrossRef Medline

Sanders SJ, Murtha MT, Gupta AR, Murdoch JD, Raubeson MJ, Willsey AJ, Ercan-Sencicek AG, DiLullo NM, Parikshak NN, Stein JL, Walker MF, Ober GT, Teran NA, Song Y, El-Fishawy P, Murtha RC, Choi M, Overton JD, Bjornson RD, Carriero NJ, et al. (2012) De novo mutations revealed by whole-exome sequencing are strongly associated with autism. Nature 485:237–241. CrossRef Medline

Schluth-Bolard C, Labalme A, Cordier MP, Till M, Nadeau G, Tevissen H, Lesca G, Boutry-Kryza N, Rossignol S, Rocas D, Dubruc E, Edery P, Sanlaville D (2013) Breakpoint mapping by next generation sequencing reveals causative gene disruption in patients carrying apparently balanced chromosome rearrangements with intellectual deficiency and/or congenital malformations. J Med Genet 50:144–150. CrossRef Medline

Schmeisser MJ (2015) Translational neurobiology in shank mutant mice—model systems for neuropsychiatric disorders. Ann Anat 200:115–117. CrossRef Medline

Schmeisser MJ, Ey E, Wegener S, Bockmann J, Stempel AV, Kuebler A, Janssen AL, Udvardi PT, Shiban E, Spilker C, Balschun D, Skryabin BV, Dieck St, Smalla KH, Montag D, Leblond CS, Faure P, Torquet N, Le Sourd AM, Toro R, et al. (2012) Autistic-like behaviours and hyperactivity in mice lacking ProSAP1/Shank2. Nature 486:256–260. CrossRef Medline

Schneider K, Seemann E, Liebmann L, Ahuja R, Koch D, Westermann M, Hübner CA, Kessels MM, Qualmann B (2014) ProSAP1 and membrane nanodomain-associated syndapin I promote postsynapse formation and function. J Cell Biol 205:197–215. CrossRef Medline

Sheng M, Hoogenraad CC (2007) The postsynaptic architecture of excitatory synapses: a more quantitative view. Annu Rev Biochem 76:823–847. CrossRef Medline

Sheng M, Kim E (2000) The shank family of scaffold proteins. J Cell Sci 113:1851–1856. Medline

Sheng M, Kim E (2011) The postsynaptic organization of synapses. Cold Spring Harb Perspect Biol 3: pii: a005678. CrossRef Medline

Sheng M, Sala C (2001) PDZ domains and the organization of supramolecular complexes. Annu Rev Neurosci 24:1–29. CrossRef Medline

Silverman JL, Yang M, Lord C, Crawley JN (2010) Behavioural phenotyping assays for mouse models of autism. Nat Rev Neurosci 11:490–502. CrossRef Medline

Soltau M, Richter D, Kreienkamp HJ (2002) The insulin receptor substrate IRSp53 links postsynaptic shank1 to the small G-protein cdc42. Mol Cell Neurosci 21:575–583. CrossRef Medline

Tang G, Gudsnuk K, Kuo SH, Cotrina ML, Rosoklija G, Sosunov A, Sonders MS, Kanter E, Castagna C, Yamamoto A, Yue Z, Arancio O, Peterson BS, Champagne F, Dwork AJ, Goldman J, Sulzer D (2014) Loss of mTOR-dependent macroautophagy causes autistic-like synaptic pruning deficits. Neuron 83:1131–1143. CrossRef Medline

Tao-Cheng JH, Yang Y, Reese TS, Dosemeci A (2015) Differential distribution of Shank and GKAP at the postsynaptic density. PLoS One 10: e0118750. CrossRef Medline

Tsien JZ, Chen DF, Gerber D, Tom C, Mercer EH, Anderson DJ, Mayford M, Kandel ER, Tonegawa S (1996) Subregion- and cell type-restricted gene knockout in mouse brain. Cell 87:1317–1326. CrossRef Medline

Tu JC, Xiao B, Naisbitt S, Yuan JP, Petralia RS, Brakeman P, Doan A, Aakalu VK, Lanahan AA, Sheng M, Worley PF (1999) Coupling of mGluR/Homer and PSD-95 complexes by the shank family of postsynaptic density proteins. Neuron 23:583–592. CrossRef Medline

Uemura T, Mori H, Mishina M (2004) Direct interaction of GluRdelta2 with shank scaffold proteins in cerebellar purkinje cells. Mol Cell Neurosci 26:330–341. CrossRef Medline

Van de Weerd HA, Bulthuis RJ, Bergman AF, Schlingmann F, Tolboom J, Van Loo PL, Remie R, Baumans V, Van Zutphen LF (2001) Validation of a new system for the automatic registration of behaviour in mice and rats. Behav Processes 53:11–20. CrossRef Medline

Wang X, Bey AL, Chung L, Krystal AD, Jiang YH (2014a) Therapeutic approaches for shankopathies. Dev Neurobiol 74:123–135. CrossRef Medline

Wang X, Xu Q, Bey AL, Lee Y, Jiang YH (2014b) Transcriptional and functional complexity of Shank3 provides a molecular framework to understand the phenotypic heterogeneity of SHANK3 causing autism and Shank3 mutant mice. Mol Autism 5:30. CrossRef Medline

Wischmeijer A, Magini P, Giorda R, Gnoli M, Ciccone R, Cecconi L, Franzoni E, Mazzanti L, Romeo G, Zuffardi O, Seri M (2011) Olfactory receptor-related duplicons mediate a microdeletion at 11q13.2q13.4 associated with a syndromic phenotype. Mol Syndromol 1:176–184. CrossRef Medline

Won H, Lee HR, Gee HY, Mah W, Kim JI, Lee J, Ha S, Chung C, Jung ES, Cho YS, Park SG, Lee JS, Lee K, Kim D, Bae YC, Kaang BK, Lee MG, Kim E (2012) Autistic-like social behaviour in Shank2-mutant mice improved by restoring NMDA receptor function. Nature 486:261–265. CrossRef Medline

Yoo J, Bakes J, Bradley C, Collingridge GL, Kaang BK (2014) Shank mutant mice as an animal model of autism. Philos Trans R Soc Lond B Biol Sci 369:20130143. CrossRef Medline

Zhu J, Shang Y, Zhang M (2016) Mechanistic basis of MAGUK-organized complexes in synaptic development and signalling. Nat Rev Neurosci 17:209–223. CrossRef Medline